Molecular Biology of the Cell
Vol. 17, 3689–3704, August 2006

Arf6-independent GPI-anchored Protein-enriched Early Endosomal Compartments Fuse with Sorting Endosomes via a Rab5/Phosphatidylinositol-3′-Kinase–dependent Machinery[D]

Manjula Kalia,* Sudha Kumari,* Rahul Chadda,* Michelle M. Hill,† Robert G. Parton,† and Satyajit Mayor*

*National Centre for Biological Sciences, UAS-GKVK Campus, Bangalore 560065, India; and †Institute for Molecular Bioscience, University of Queensland, Queensland 4072, Australia

Submitted October 25, 2005; Revised April 21, 2006; Accepted May 25, 2006
Monitoring Editor: Jean Gruenberg

In the process of internalization of molecules from the extracellular milieu, a cell uses multiple endocytic pathways, consequently generating different endocytic vesicles. These primary endocytic vesicles are targeted to specific destinations inside the cell. Here, we show that GPI-anchored proteins are internalized by an Arf6-independent mechanism into GPI-anchored protein-enriched early endosomal compartments (GEECs). Internalized GPI-anchored proteins and the fluid phase are first visualized in GEECs that are acidic, primary endocytic structures, negative for early endosomal markers, Rab4, Rab5, and early endosome antigen (EEA)1. They subsequently acquire Rab5 and EEA1 before homotypic fusion with other GEECs, and heterotypic fusion with endosomes containing cargo from the clathrin-dependent endocytic pathway. Although, the formation of GEECs is unaffected by inhibition of Rab5 GTPase and phosphatidylinositol-3′-kinase (PI3K) activity, their fusion with sorting endosomes is dependent on both activities. Overexpression of Rab5 reverts PI3K inhibition of fusion, providing evidence that Rab5 effectors play important roles in heterotypic fusion between the dynamin-independent GEECs and clathrin- and dynamin-dependent sorting endosomes.

INTRODUCTION

A cell uses multiple endocytic pathways for the uptake of molecules from the extracellular milieu (Mukherjee *et al*., 1997; Conner and Schmid, 2003). The better characterized pathways are mediated by clathrin- and caveolae-coated endocytic invaginations and require dynamin activity to be severed from the plasma membrane (Damke *et al*., 1994; Hinshaw and Schmid, 1995; Henley *et al*., 1998; Oh *et al*., 1998). There also seem to be one or more clathrin-independent pathways where dynamin is required, for example, the pathway for internalization of the interleukin (IL)-2 receptor subunits (Lamaze *et al*., 2001). In addition, there are a growing number of dynamin-independent endocytic processes that serve as internalization routes for a number of cell surface proteins, including lipid-linked proteins, such as GPI-anchored proteins (Lamaze and Schmid, 1995; Conner and Schmid, 2003; Nichols, 2003; Mayor and Riezman, 2004; Naslavsky *et al*., 2004; Kirkham and Parton, 2005).

This article was published online ahead of print in *MBC in Press* (http://www.molbiolcell.org/cgi/doi/10.1091/10.1091/mbc.E05–10–0980) on June 7, 2006.

[D] The online version of this article contains supplemental material at *MBC Online* (http://www.molbiolcell.org).

Address correspondence to: Satyajit Mayor (mayor@ncbs.res.in).

Abbreviations used: EEA1, early endosomal antigen; GEEC, GPI-anchored protein-enriched early endosomal compartment; PI3P, phosphatidylinositol 3′-phosphate; PKC, protein kinase C; WT, wortmannin.

GPI-anchored proteins are internalized via a dynamin, caveolin, and clathrin-independent pathway that is also responsible for the entry of a sizable fraction of the fluid phase in a number of cell types (Fivaz *et al*., 2002; Sabharanjak *et al*., 2002; Guha *et al*., 2003; Kirkham *et al*., 2005). GPI-anchored proteins and the fluid phase enter the cell via tubular invaginations at the cell surface, into compartments termed GPI-anchored protein-enriched early endosomal compartments (GEECs) (Sabharanjak *et al*., 2002; Kirkham *et al*., 2005). At early times, these structures are largely devoid of cargo from the clathrin-dependent pathway. Besides a requirement for the small GTPase cdc42, very little is known about the molecular players that govern the formation and trafficking of GEECs. Much less is known about the detailed endocytic itinerary of these pathways (Lamaze and Schmid, 1995; Mayor and Riezman, 2004).

After internalization, endocytic vesicles derived from the plasma membrane seem to map out distinct fates. Clathrin-coated vesicles eventually fuse with sorting endosomes (Mukherjee *et al*., 1997). Sorting endosomes are characterized by their ability to undergo small GTPase Rab5-dependent homotypic fusion (Zerial and McBride, 2001). These endosomes are also the site for sorting recycling cargo from lysosomally directed material (Gruenberg and Maxfield, 1995).

After internalization via GEECs, GPI-anchored proteins, such as the folate receptor (FR-GPI) and decay accelerating factor, eventually reach the pericentriolar recycling endosomal compartment in Chinese hamster ovary (CHO) cells (Chatterjee and Mayor, 2001; Sabharanjak *et al*., 2002), suggesting that GEECs may fuse with sorting endosomes or at

least deliver their cargo to endosomes derived from the clathrin-mediated pathway. In baby hamster kidney (BHK) cells, GPI-anchored proteins are delivered to early endosomal antigen (EEA)1-positive endosomes, en route to late endosomes (Fivaz *et al.*, 2002). These trafficking itineraries suggest there might be a cell type-dependent plasticity in intracellular destination of these proteins (Mayor and Riezman, 2004). The pathways and molecular players involved in mediating these trafficking steps are not known.

Several factors can influence the exact nature of the pathway that GPI-anchored proteins follow (Sharma *et al.*, 2002). As reviewed recently, these pathways can be understood in terms of the nature of lateral associations that GPI-anchored proteins can make (Mayor and Riezman, 2004). The uptake of cross-linked (usually by artificial means) GPI-anchored proteins takes place via caveolae (Anderson *et al.*, 1992; Parton *et al.*, 1994). It also seems that specific lateral associations of GPI-anchored proteins with other plasma membrane components could drastically influence their precise pathway of internalization. In the case of GPI-anchored prion proteins in neuronal cells, their amino-terminal domain specifies clathrin-pit localization, and this might be augmented by association of the prion protein with metal ions (Pauly and Harris, 1998; Sunyach *et al.*, 2003). In recent studies, it has been shown that GPI-anchored prion protein (PrP^{C}) is enriched in caveolae at the plasma membrane, and a caveolar uptake mechanism for PrP^{C} and its conversion to PrP^{sc} was proposed. However, the study demonstrated that PrP^{C} followed a different endocytic route than other GPI-anchored proteins, such as CD59, which showed no enrichment in caveolae (Peters *et al.*, 2003). Other instances of such protein-specific modulation are binding of a complex of the urokinase-type plasminogen activator (uPA) and its GPI-anchored uPA receptor to the α-2 macroglobulin receptor/low-density lipoprotein receptor-related protein (Nykjaer *et al.*, 1992; Conese *et al.*, 1995); and GPI-anchored CD14, which interacts with bacterial lipopolysaccharide (LPS) bound to the plasma-LPS-binding protein (Poussin *et al.*, 1998; Triantafilou *et al.*, 2001). In the absence of lateral associations of the type described above, or cross-linking and internalization through the caveolar/raft-dependent pathway (Nabi and Le, 2003), GPI-anchored proteins seem to be selectively internalized through a dynamin-independent pathway (Fivaz *et al.*, 2002; Sabharanjak *et al.*, 2002; Guha *et al.*, 2003). It has been recently shown that the nanoscale organization of GPI-anchored proteins on the plasma membrane also influences their endocytic pathways (Sharma *et al.*, 2004).

In a variety of mammalian cell types (Skretting *et al.*, 1999; Ricci *et al.*, 2000; Fivaz *et al.*, 2002) and in *Drosophila* hemocytes (Guha *et al.*, 2003), GPI-anchored proteins continue to be internalized even when dynamin activity is inhibited. GPI-anchored proteins are then delivered to Rab5-negative GEECs.

Recently, Nichols (2002) has shown some overlap of caveolin-1 (Cav1)-green fluorescent protein (GFP) with endogenous GPI-anchored protein CD59-labeled structures and internalized 10K dextran (Dex) at relatively late times in structures called caveosomes. From these studies, however, it was not clear whether endocytosed GPI-anchored proteins were delivered to caveosomes. Furthermore, endocytic trafficking of markers found in caveosomes (e.g., cholera toxin B; CTxB) was not affected when caveolin-1 was depleted by RNAi treatment and so it is unlikely that Cav1 forms an essential component of the relevant membrane trafficking machinery (Nichols, 2002). In this context, it is important to note that caveolin-coated vesicles seem to follow a distinct intracellular itinerary. Examining transport of the caveolar protein Cav1 and two cargo complexes, simian virus 40 (SV40) and cholera toxin, investigators have shown that caveolin-coated vesicles are targeted to Rab5-dependent early endosomes and form distinct and stable membrane domains (Pelkmans *et al.*, 2004). In early endosomes, the low pH selectively allowed the toxin to diffuse out of the caveolar domains into the surrounding membrane, whereas the virus remained trapped. Cholera toxin finally reaches the Golgi from the early endosome, whereas SV40 transits independently along microtubules to the endoplasmic reticulum (ER) (Pelkmans *et al.*, 2004). These two ligands, SV40 and cholera toxin, that are specific for the caveolar pathway, can also follow a caveolin- and dynamin-independent endocytic pathway in cells lacking caveolae and Cav1 and -2 (Damm *et al.*, 2005; Kirkham *et al.*, 2005). Cholera toxin continues to be internalized via tubular carriers that are also enriched for GPI-anchored proteins (Kirkham *et al.*, 2005), whereas SV40 enters a pH-neutral compartment that does not fuse with sorting endosomes but transits onto the ER (Damm *et al.*, 2005).

Many steps of the endocytic transport, such as vesicle formation, motility, tethering, and fusion, are tightly regulated by small GTPases such as Rab proteins, localized to distinct cellular compartments (Simons and Zerial, 1993; Mellman, 1996; McLauchlan *et al.*, 1998; Simonsen *et al.*, 1998). These proteins cycle between an active, GTP-bound, and an inactive, GDP-bound state, and engage molecular effectors to carry out their function (Pfeffer, 2001; Zerial and McBride, 2001). In addition to the Rab family of proteins, the Arf GTPases (especially Arf6) have also been recently shown to play an important role in endocytic trafficking (Brown *et al.*, 2001; Donaldson, 2003). Studies in HeLa cells suggest that Arf6 is a key player in regulating the endosome dynamics of a dynamin-independent pathway wherein GPI-anchored proteins are internalized into Arf6-labeled compartments, which also contain endocytosed membrane proteins, myosin heavy chain I (MHCI), and Tac (Naslavsky *et al.*, 2003, 2004). In this Arf6-associated pathway, the GTP hydrolysis cycle of Arf6 regulates internalization, fusion with sorting endosomes, and/or recycling of endosomes derived from this pathway (Radhakrishna and Donaldson, 1997; Naslavsky *et al.*, 2003) without affecting the clathrin-dependent pathway.

In this article, we have addressed three issues about the GEEC pathway: 1) the role of Arf6 in the generation of GEECs; 2) pH and fusion capacity of earliest detectable GEECs; and 3) the role of Rab5 and two effectors of the Rab5 subsystem, EEA1 and PI3K, in the formation and consumption of GEECs.

MATERIALS AND METHODS

Reagents, cDNAs, and Antibodies

Unless otherwise mentioned all chemicals and reagents were obtained from Sigma-Aldrich (Hyderabad, India). Folate-free Ham's F-12 (F^{-} HF-12), and sodium fluoride were obtained from Hi-Media (Mumbai, India); FuGENE 6 was from Roche Molecular Biochemicals (Nicholas Piramal India, Mumbai, India). All fluorescent reagents and probes were from Invitrogen (Eugene, OR) or GE Healthcare (Little Chalfont, Buckinghamshire, United Kingdom) and have been described previously (Mayor *et al.*, 1998; Chatterjee *et al.*, 2001; Sabharanjak *et al.*, 2002). Monoclonal antibodies against EEA1 and Rab5 were from Signal Transduction Laboratories (Becton-Dickinson, Singapore). Anti-hemagglutinin (HA) antibodies were from Cell Signaling Technology (Beverly, MA); anti-GFP antibodies were from Bangalore Genei (Bangalore, India). Goat anti-mouse Fc-specific secondary antibody was from Jackson ImmunoResearch Laboratories (West Grove, PA) and was coupled to either Alexa 488 or Alexa 568 according to manufacturer's instructions. Wild-type (wt)-GFP-Rab5, dominant-negative (DN)-GFP-Rab5, dominant-active (DA)-GFP-Rab5, and wt-GFP-Rab4 were a gift from Dr. Marino Zerial (Max-Plank Institute of Molecular Cell Biology and Genetics, Dresden, Germany). HA-

and GFP-tagged Arf6-DA, -(DN), and -wt constructs were a gift from Dr. J. Donaldson (National Institutes of Health, Bethesda, MD).

Cell Labeling and Other Treatments

CHO cells stably expressing GFP-GPI and monomeric cyan fluorescent protein (CFP)-GPI were generated as described previously and maintained in HF-12, 10% serum (Sabharanjak *et al*., 2002). All CHO cell lines were maintained as described previously (Mayor *et al*., 1998). Primary mouse embryonic fibroblasts (MEFs) were obtained from 13.5-d-old embryos from either Cav1 knockout or wild-type mice (Kirkham *et al*., 2005). Immortalization to produce Cav1−/− cell lines was achieved by passaging cells according to published procedures (Razani and Lisanti, 2001). MEFs, BHK, and HeLa cells were maintained in DMEM, 10% serum. Cells were incubated with endocytic tracers for indicated times in labeling medium (HF-12 or DMEM, 10% serum). For FR-GPI labeling, fluorescent derivatives of folic acid, fluorescein-conjugated folic acid (N^{α}-pteroyl-N^{ε}-(4′-fluorescein-thiocarbamoyl)-L-lysine; PLF), and a rhodamine-labeled analogue of folic acid (N^{α}-pteroyl-N^{ε}-(4′-rhodamine-thiocarbamoyl)-L-lysine; PLR) were used. Fluorescently labeled Fab fragments of Mov18, Fab fragments of anti-GFP antibody, and transferrin (Tf) were obtained as described previously (Mayor *et al*., 1998; Chatterjee *et al*., 2001), fluorescein isothiocyanate (FITC)-Dex or tetramethyrhodamine (TMR)-Dex (1 mg/ml) was used to mark the fluid phase. Fluorescently labeled CTxB was used at 2 μg/ml. No difference in the endocytic properties and distribution of CTxB was seen at a range of 0.5–10 μg/ml. After incubation with labeled tracers, excess label was washed off with medium1 (M1; Mayor *et al*., 1998). To visualize the endosomal distribution of the fluorescent tracers, cells were cooled on ice, and cell surface label (fluorescently labeled Tf) was removed by incubating cells in ice-cold ascorbate buffer pH 4.5; surface fluorescence from labeled Fab fragments or intact antibody against GPI-anchored proteins was removed by phosphatidylinositol-specific phospholipase C treatment. Fluoresecently labeled CTxB was removed by washing with a low pH buffer (100 mM glycine, 10 mM magnesium acetate tetrahydrate, and 50 mM potassium chloride 50, pH 2.2). Cells were fixed with 2% paraformaldehyde. To detect intracellular antigens they were permeabilized with 0.4% Tween 20 in M1/bovine serum albumin buffer and stained with appropriate primary and secondary antibodies. Cells were transiently transfected using FuGENE 6 according to manufacturer's instructions. Transfected cells were identified by CFP, GFP fluorescence or by immunostaining of epitope-tagged proteins expressed in cells using appropriate anti-epitope antibodies. Aluminum fluoride treatment was carried out by treating cells with a mixture of 10 mM NaF and 10 μM $AlCl_3$ for 30 min at 37°C.

Measurement of pH in GEECs and Sorting Endosomes

The estimation of the organelle pH was based on a ratiometric assay using fluorescein as an indicator of pH (Maxfield, 1989), FITC-Dex and TMR-Dex as fluid phase probes, and Cy5-Tf as a sorting endosomal marker. For this purpose, GEECs were identified as fluid endosomes that are not colocalized with Cy5-Tf, whereas the sorting endosomes were identified as endosomes that contain both fluid and Tf. FITC-Dex at a concentration of 1 mg/ml is a reliable marker of GEECs in CHO cells (Sabharanjak *et al*., 2002). That the compartments marked by endocytosed FITC-Dex represent GEECs was also independently ascertained for these experiments by examining colocalization with PLR; colocalization between FITC-Dex and PLR was close to 90%. After a 2-min pulse, cells were incubated on ice with 10 μM nigericin in different pH buffers ranging from 4 to 9 as indicated. The cells were left in this medium until imaging, and the fluorescence ratio of FITC to TMR at different equilibrated pHs was calculated in individual endosomes. The mean and SE of the distribution of individual endosome ratios of FITC to TMR were obtained at different pHs and plotted to obtain a calibration curve. The pH of GEECs and sorting endosomes were estimated by comparing values obtained for the fluorescence ratios of FITC to TMR in the respective compartments to the calibration curve. The experiment was repeated three times with similar results. The experiment was also performed after mild fixation of cells (2% paraformaldehyde for 2 min on ice) and gave identical results.

Endocytic Uptake Assays

For quantitative measurements of endocytosis of fluid phase, FR-GPI and Tf, cells were incubated with fluorescently conjugated reagents for 2, 5, or 10 min and extensively washed before imaging. Endocytic uptake of all probes was quantified at low magnification (20×, 0.75 numerical aperture [NA]) as described previously (Chatterjee *et al*., 2001).

High-Resolution Imaging and Image Processing

High-resolution wide-field images were collected using Nikon TE 200 inverted microscope equipped with 60×, 1.4 NA objective, a mercury arc illuminator (Nikon, Tokyo, Japan), and a cooled charge-coupled device (CCD) camera (TEK-512B CCD detector mounted in a MicroMax Camera, Princeton Instruments, NJ) controlled by MetaMorph software (Molecular Devices, Downingtown, PA). Optimized dichroics, excitation, and emission filters were used as described previously (Chatterjee *et al*., 2001). Confocal imaging was carried out using Zeiss 510 Meta laser scanning microscope (Carl Zeiss India Pvt. Ltd., Bangalore, India).

We found the high-resolution, wide-field microscopy system best suited for quantification and detection of a range of signals of endocytosed probes, compared with confocal detection systems, due to its high sensitivity. First, the high dynamic range (16 bit; full depth, ~12 bit working range for dimly labeled cells, after accounting for intrinsic autofluorescence in cells) afforded by the wide-field system made it possible to collect images of endocytosed probes from both low- and high-expressing cells, with the same exposure settings. In the case of colocalization experiments, it is important to have access to the high dynamic range so that colocalization is not artificially reduced due to thresholding of signal from low signal levels. Second, confocal imaging in most cases reported artificially low colocalization indexes, due to the lack of sensitivity of the confocal detection system. However, in all cases the trends observed were preserved. For example, using this system we obtain average colocalization indices of 80% using two color probes for the same receptors; confocal imaging reports a much lower index, sometimes <40%, if the intensities of the two probes were not matched.

Quantitative Colocalization Analysis

The quantification of colocalization of endocytic markers in high-resolution wide-field images was determined using established software routines "spots," capable of identifying and quantifying the intensity of each endosomes, followed by "coloc" to determine the extent of colocalization of individual endosomes with identified endosomes in a reference image (Dunn *et al*., 1989; Mayor *et al*., 1993; Ghosh *et al*., 1994). The criteria outlined below were applied to images obtained from CHO cells either untransfected or transfected with HA-Arf6 wt, GFP-Rab5 wt; stained for EEA1; and/or labeled with endocytic tracers against FR-GPI and TfR for different time points at 37°C. High-resolution images of cells were obtained using a 60× 1.4 NA objective on a wide-field microscope at a pixel resolution of 0.15 μm/pixel. The images were corrected for background fluorescence using the "Produce background correction image procedure" in MetaMorph image analysis software using the following parameters suitable for producing a local background image and at the same time preserving the intensity of the endosomes (box size = 30 × 30 pixels; subsample ratio = 10; percentile = 0.2).

The background corrected images were then processed through spots to identify endosomes using parameters defined by pixels above a threshold (set by inspection for each image) and area (min = 3 pixel, max = no upper limit). A trimming procedure was applied to isolate and segregate individual endosomes based on the inclusion of pixels with intensities greater than 0.3 of maximal intensity within a unit of connected pixels having intensity greater than the set threshold. This was achieved by an iterative procedure using a step size (0.01) for each iteration. This limits the number of iterations of the trimming procedure. The resultant image consists of a background subtracted image containing a set of well defined spots or "endosomes" in terms of net intensity per spot and total pixel area per spot.

The two spotted images of different fluorophore-labeled endocytic tracers are matched up against each other to identify the endosomes wherein the two endocytic tracers are colocalized. Endosomes in a tracer image (e.g., FR-GPI-containing endosomes) are compared with endosomes in a "reference image" (e.g., Tf-containing endosomes) using coloc, and endosomes with 50% or more area overlap are considered as colocalized. The resultant image displays all the spots that are colocalized using a particular "reference-tracer" image pair.

Cellular outlines in this image were traced on the phase contrast image of the cell, and the net intensity of each fluorophore per cell was calculated in the spotted as well as the coloc images using procedures outlined in MetaMorph. The colocalization index was then calculated as the ratio of the net intensity of a probe within a cell in the coloc image to the net intensity of the probe within the same cell in a spots image. Colocalization index was expressed as a percentage of the colocalized intensity to the total intensity of the probe in endosomes identified in each cell. Mean and SEM of the colocalization index were obtained from two to five independent experiments from at least 10–15 cells in each experiment, as described previously (Sabharanjak *et al*., 2002).

RESULTS

Arf6 Is Not a Specific Marker for GEECs in CHO Cells

Studies in HeLa cells have shown that ectopically expressed Arf6 outlines the clathrin-independent internalization pathway that operates on plasma membrane proteins that lack clathrin localization motifs, such as MHCI and IL-2 receptor α subunit (Tac) (Naslavsky *et al*., 2003), as well as GPI-anchored proteins (Naslavsky *et al*., 2004). Furthermore, in HeLa cells the tubular Arf6 recycling compartment is distinct from the transferrin recycling endosome; early endosomes containing MHCI and CD59 (GPI-anchored protein) colocalize with overexpressed Arf6, whereas endosomes

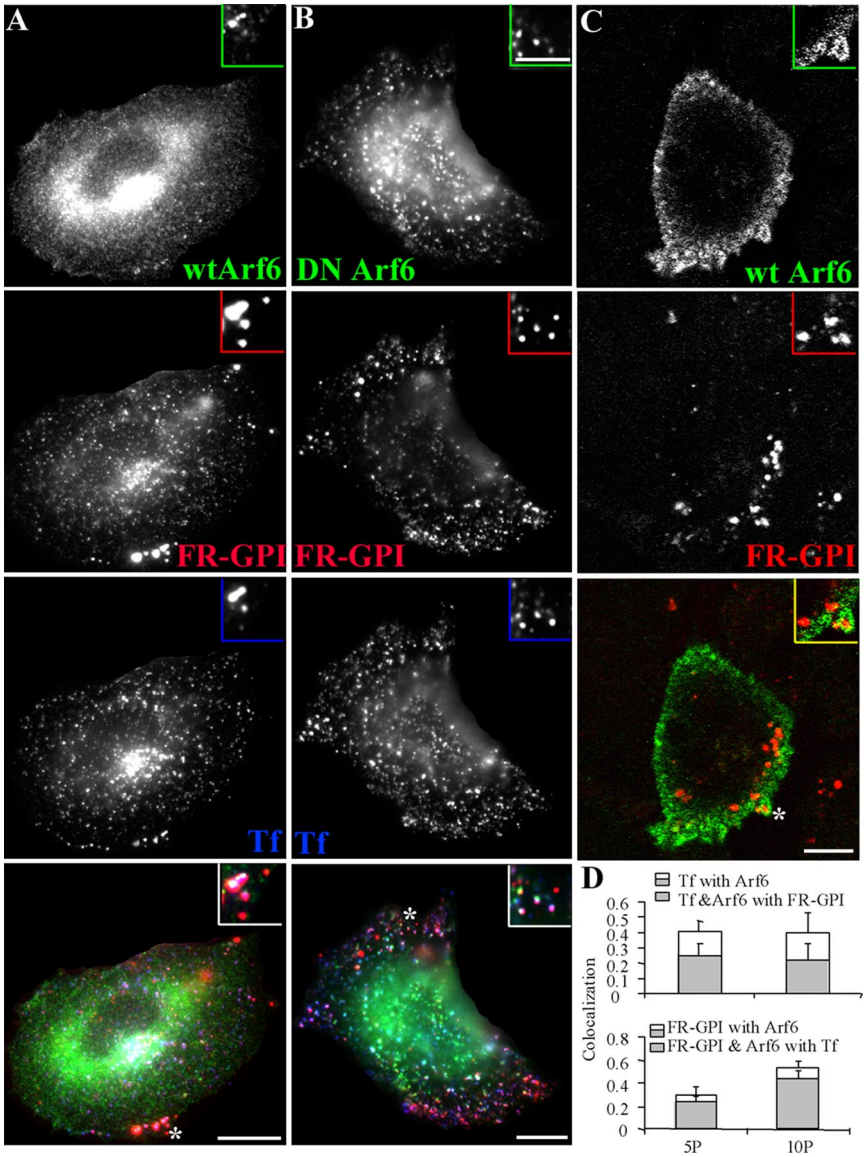

Figure 1. Arf6 is not a specific marker of the GEEC pathway in CHO cells. CHO cells transfected with HA-tagged wt-Arf6 (A and C) or HA-tagged DN-Arf6 (T27N; B) were given a 10-min pulse (A and B) of Cy5-labeled Fab-fragment of anti-folate receptor antibody Mov18 (Cy5-Fab-Mov18; red in A–C) and Cy3-Tf (blue in A and B) or a 2-min pulse of Cy5-Fab-Mov18 (C), fixed, and stained with Alexa 488-labeled anti-Fc-fragment antibody against the HA-tag (green). The cells were imaged on a wide-field microscope (A and B) or a confocal microscope (C) as described in text. Images are presented as gray scales for individual colors, and pseudocolored as indicated before being merged. Insets show a magnified view of the region corresponding to the asterisk (*). Note that Tf-containing endosomes exhibit significant colocalization with Arf6 (pink structures), whereas the GPI-anchored proteins containing endosomes only show an occasional overlap with Arf6 in structures also containing Tf (pinkish white). At 2 min, most of the GEECs are not in any Arf6 structures (C). (D) Histogram showing extent of overlap between Arf6 and Tf endosomes (top l), and Arf6 and FR-GPI endosomes (bottom) at different pulse times (5P, 5 min; and 10P, 10 min). The shaded area enclosed in the open bar indicates the fraction of Tf-positive endosomes (D, top) that colocalized with both Arf6 and FR-GPI, and of FR-GPI-positive endosomes (D, bottom) that colocalized with both Arf6 and Tf. Bar, 10 μm and 5 μm (inset).

containing cargo from the clathrin pathway, such as Tf, do not (Naslavsky *et al*., 2004).

The effects and distribution of Arf6 seem to vary between cell types. In contrast to ectopically expressed Arf6 in HeLa cells, endogenous Arf6 seems to mark the clathrin-dependent endocytic pathway in CHO cells (D'Souza-Schorey *et al*., 1995). Recently, studies have shown that Arf6 also plays a major role in clathrin-mediated endocytosis by directly controlling the assembly of the AP-2/clathrin coat (Paleotti *et al*., 2005; Tanabe *et al*., 2005). Arf6 has also been shown to be involved in recycling of endocytic membranes via the exocyst effector complex (Prigent *et al*., 2003). It also regulates dynamin and clathrin-dependent endocytosis of E-cadherin at adherens junctions (Palacios *et al*., 2002). In addition, Arf6 activity has been consistently associated with formation of actin-based plasma membrane protrusions (Radhakrishna and Donaldson, 1997; Song *et al*., 1998; Honda *et al*., 1999).

Indeed, in CHO cells transfected with HA-tagged wild-type Arf6 (HA-wtArf6) or HA-tagged constitutively inactive Arf6 (T27N mutant, DN-Arf6), Tf-containing endosomes show a high degree of colocalization with Arf6 (Figure 1, A, B, and D). Quantitatively, ~45% of Tf-containing endosomes were colocalized with Arf6, 5 min postinternalization (Figure 1D, top). However, endosomes containing fluid and GPI-anchored proteins internalized for short times (2 min; Figure 1C) were not associated with Arf6-labeled structures. Less than 15% of these structures colocalized with Arf6 as determined from a qualitative inspection of confocal images (Figure 1C) of >500 GPI-anchored protein-containing endosomes in 20 cells. There was also no association of wt-Arf6 or DN-Arf6 with these endosomes at later times (Figure 1, A and B, respectively). GPI-anchored protein containing endosomes that colocalized with Arf6 also contained Tf (Figure 1, A and D); 80% of Arf6-positive GPI-anchored protein-containing endosomes were colocalized with Tf (Figure 1D, shaded bars, bottom). This implies that Arf6 is detected on GPI-anchored protein-containing endosomes only after they acquire Tf internalized via clathrin-derived pathways.

In HeLa cells, expression of constitutively active Arf6 (DA-Arf6 Q67L mutant) increases uptake of MHCI, Tac, and GPI-anchored proteins by almost twofold (Naslavsky *et al*., 2003, 2004), and these proteins accumulate in en-

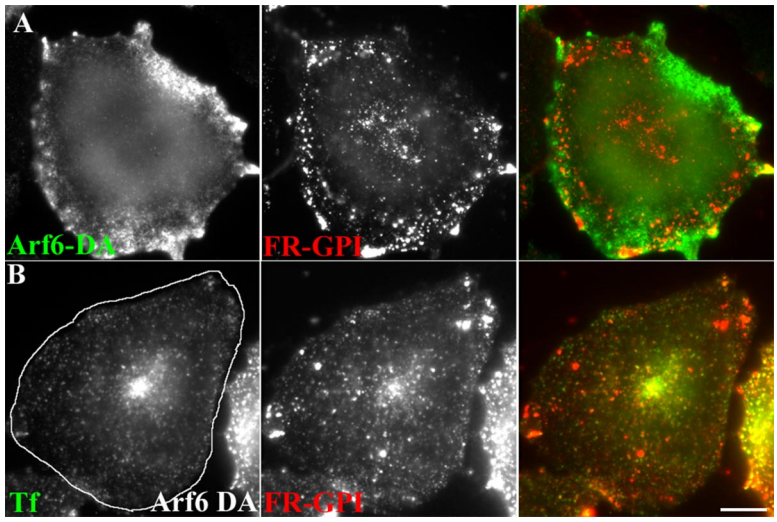

Figure 2. DA-Arf6 does not block fusion between GEECs and sorting endosomes and allows delivery of GPI-anchored proteins to the recycling endosome. (A) CHO cells transfected with HA-tagged DA-Arf6 (green) were given a 10-min pulse of Cy5-Fab-Mov18 (red). Endosomes containing FR-GPI show some overlap with membrane ruffles of DA-Arf6, however a significant fraction of Cy5-Fab-Mov18 labeled endosomes are not colocalized with DA-Arf6. (B) CHO cells transfected with GFP-DA-Arf6 (outlined cell) were given a 20-min pulse of Alexa 568-Tf (green) and Cy5-MOv18 Fab (red). Note fusion of endosomes of Tf and FR-GPI in the periphery of DA-Arf6 expressing cells. FR-GPI and Tf are also delivered to the pericentriolar recycling compartment in transfected cells. Bar, 10 μm.

larged phosphatidylinositol bisphosphate-enriched vacuoles; there is an inhibition of fusion with clathrin cargo-containing endosomes, and further trafficking of both membrane and fluid is blocked in these cells (Naslavsky *et al*., 2003). By contrast, trafficking and degradation of molecules endocytosed via the clathrin-mediated pathway are unaffected in HeLa cells expressing DA-Arf6 (Naslavsky *et al*., 2003).

In CHO cells, overexpression of wt-Arf6, DA-Arf6, or DN-Arf6 had no significant effect on uptake of FR-GPI as well as the fluid phase (Supplemental Figure 1). In contrast, DA-Arf6 inhibited Tf uptake (Supplemental Figure 1), consistent with previous studies (D'Souza-Schorey *et al*., 1995, 1998; Tanabe *et al*., 2005). Expression of DA-Arf6 (Q67L mutant) generates actin-rich surface protrusions in CHO cells (our unpublished data), and under these conditions DA-Arf6 decorates structures containing internalized GPI-anchored proteins, often coincident with the actin-rich protrusions (Figure 2A). Frequently, these structures also contain internalized Tf, consistent with their identity as macropinocytic membrane engulfments carrying "nonspecific" membrane cargo (our unpublished data).

In contrast to HeLa cells (Naslavsky *et al*., 2003), in CHO cells overexpressing DA-Arf6, endocytosed GPI-anchored proteins continued to fuse with sorting endosomes and acquire endocytosed Tf cargo, and they are delivered to recycling endosomes with apparently unaltered kinetics (Figure 2B). These observations suggest that Arf6 may not function to regulate internalization of proteins brought into the cell via the GEEC pathway in CHO cells. Furthermore, unlike in HeLa cells where DA-Arf6 prevents delivery of membrane components to the tubular recycling compartments and fusion with clathrin-derived endosomes, Arf6 inactivation is not required for delivery of GPI-anchored proteins to the tubular recycling compartment in CHO cells.

Aluminum Fluoride (AlF) Inhibits the GEEC Pathway

AlF treatment leads to acute activation of transfected Arf6, resulting in protrusive structures, changes in cortical actin, and mimics DA-Arf6 mutant Q67L (Radhakrishna *et al*., 1996). These AlF-induced membrane protrusions are sites of enhanced macropinocytosis in HeLa cells. There is a clear change in the pattern of uptake and recycling of membrane and fluid within membrane protrusions in AlF-treated and Arf6-transfected cells (Radhakrishna *et al*., 1996). However, AlF treatment in untransfected HeLa cells did not seem to alter uptake of the pattern of fluid phase (Radhakrishna *et al*., 1996). In contrast, treatment of untransfected CHO cells with AlF leads to a significant inhibition in uptake of fluid and GPI-anchored proteins at concentrations where Tf uptake is unaffected (Supplemental Figure 2, A and C). In AlF-treated cells, only when Arf6 is ectopically overexpressed, internalization of fluid (our unpublished data) and GPI-anchored proteins (Supplemental Figure 2B) is observed. Under these conditions there is significant colocalization between ectopically expressed Arf6- and GPI-anchored protein-containing endosomes (Supplemental Figure 2B). Together, these results suggest that in the presence of AlF, overexpression of Arf6 may be activating a parallel pathway for internalization of GPI-anchored proteins and the fluid phase, similar to that seen in Arf6-transfected HeLa cells (Radhakrishna *et al*., 1996; Naslavsky *et al*., 2003).

One explanation for these results may be a consequence of having two types of endocytic mechanisms for the internalization of nonclathrin pathway-targeted membrane components. Indeed, comparison of endocytosis in HeLa and CHO (or BHK) cells reveals that uptake of the fluid phase and GPI-anchored proteins occur with different kinetics and extents. Uptake of fluid phase (Supplemental Figure 3) and GPI-anchored proteins (our unpublished data) into GEECs devoid of Tf, seems more efficient in CHO and BHK cells than in HeLa cells. Most of the fluid-filled endosomes in HeLa cells overlap with endocytosed Tf at 2 min; 60–80% of fluid-filled endosomes in HeLa cells colocalized with Tf, whereas 50–70% of the endosomes in CHO and BHK cells were independent of Tf (our unpublished data).

GPI-anchored Proteins Are Internalized into Acidic Primary Endocytic Vesicles, before Fusion with Sorting Endosomes

We next addressed the nature of the endocytic process responsible for internalization of GPI-anchored proteins and the fluid phase into GEECs. In CHO cells stably expressing GPI-anchored GFP (Sabharanjak *et al*., 2002), newly internalized fluid phase (between 0 and 2 min) is localized to endocytic vesicles that are almost exclusively marked by GFP-GPI but not endocytosed Tf (Supplemental Figure 4). This suggests that the process of GEEC formation is constitutive, bringing into the cell both fluid phase and membrane cargo

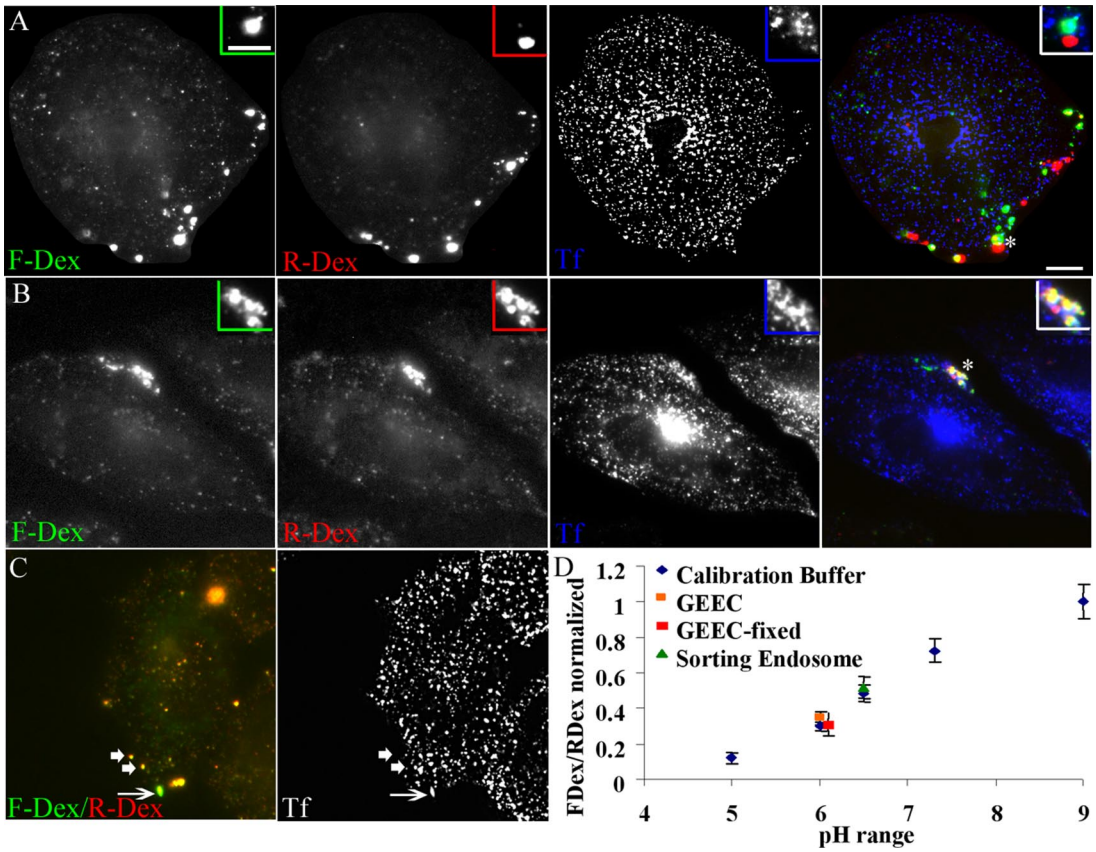

Figure 3. Acidic GEECs are formed from fusion of primary endocytic vesicles. (A and B) CHO cells were pulsed for 2 min at 37°C with FITC-Dex (green) followed by a 30-s wash and a 2-min pulse of TMR-Dex (red), in the presence of Cy5-Tf (blue). Cells were either directly fixed (A) or alternately washed and chased for another 2 min (B) before imaging. Note that the endosomes of FITC-Dex (green, first pulse) are completely separate from those of TMR-Dex (red, second pulse) and are also not colocalized with Tf endosomes (blue; A). After a further chase, fluid endosomes fuse with each other and also with Tf-containing sorting endosomes (B). Insets show a magnified view of the region corresponding to the asterisk (*). Bar, 10 μm and 5 μm (inset). (C) Measurement of endosomal pH. Cells were given a 2-min pulse of FITC-Dex, TMR-Dex, and Cy5-Tf. Note that fluid endosomes that have fused with Tf-containing sorting endosomes (arrow) have a brighter green fluorescence, indicating a higher pH of the endosome compared with fluid endosomes that are not colocalized with Tf (arrowheads). (D) pH calibration. Cell were pulsed for 2 min with a mixture of FITC-Dex and TMR-Dex to label early endosomes, and subsequently equilibrated with a range of different buffer pHs in the presence of 10 μM nigericin to obtain a calibration of the ratio of FITC-Dex to TMR-Dex fluorescence against buffer pHs. This is represented as the ratio of FITC-Dex to TMR-Dex fluorescence normalized to the value at pH 9.0. pH of GEECs (fluid endosomes not colocalized with Tf-containing endosomes; data point in orange) was close of 6, whereas the pH of sorting endosomes (fluid endosomes fused with transferrin; data point in green) was close to 6.5, indicating that GEECs are much more acidic than the sorting endosomes. The experiment was also performed after mild fixation of cells (2 min on ice), with identical results; pH of the GEECs in fixed cells (indicated by data point in red) was also close to 6.

without the requirement of ligand binding for stimulating uptake of the membrane cargo.

To ascertain whether the earliest GEECs detected were formed by fusion between many primary endocytic events or whether the GEECs themselves had characteristics of primary endocytic vesicles, we examined the ability of newly formed GEECs (2-min structures) to access a second pulse of cargo from the cell surface. For this purpose, we first delivered a short 2-min pulse of FITC-Dex and followed this up with a second pulse of a differently tagged fluid phase marker, TMR-Dex. We chose 2 min as the pulse time because at times shorter than 2 min, the only difference was that fewer endosomes were detected per cell. We then examined colocalization between the two probes. As a control, when the probes are pulsed together, they seem completely colocalized (Figure 3C). However, if there is a 30-s gap between the two pulses, the first pulse is almost completely segregated from the first pulse (Figure 3A). When the endocytosed probes are chased for an additional 2 min, there is significant mixing between the two different-colored Dex-labeled endosomes (Figure 3B). These results are consistent with GEECs being generated from detectable primary endocytic events that subsequently fuse with preexisting endosomes inside the cell.

Initially, the endosomes populated by the second pulse (2 min) of endocytosed TMR-Dex label are segregated from Tf-containing sorting endosomes derived from the clathrin-dependent pathway. However, at this time there is significant mixing of endosomes derived from the first pulse (FITC-Dex) with endosomes carrying cargo (Tf) from the clathrin-dependent pathway (Figure 3A; also see Figures 5–7 and Sabharanjak *et al.*, 2002). After the chase period when the two Dex pulses seem colocalized, these endosomes are positive for endocytosed Tf, suggesting an extensive mixing between the early endosomal organelles of these two endosomal systems.

To further characterize GEECs that were not fused with Tf-containing sorting endosomes, we measured the pH of

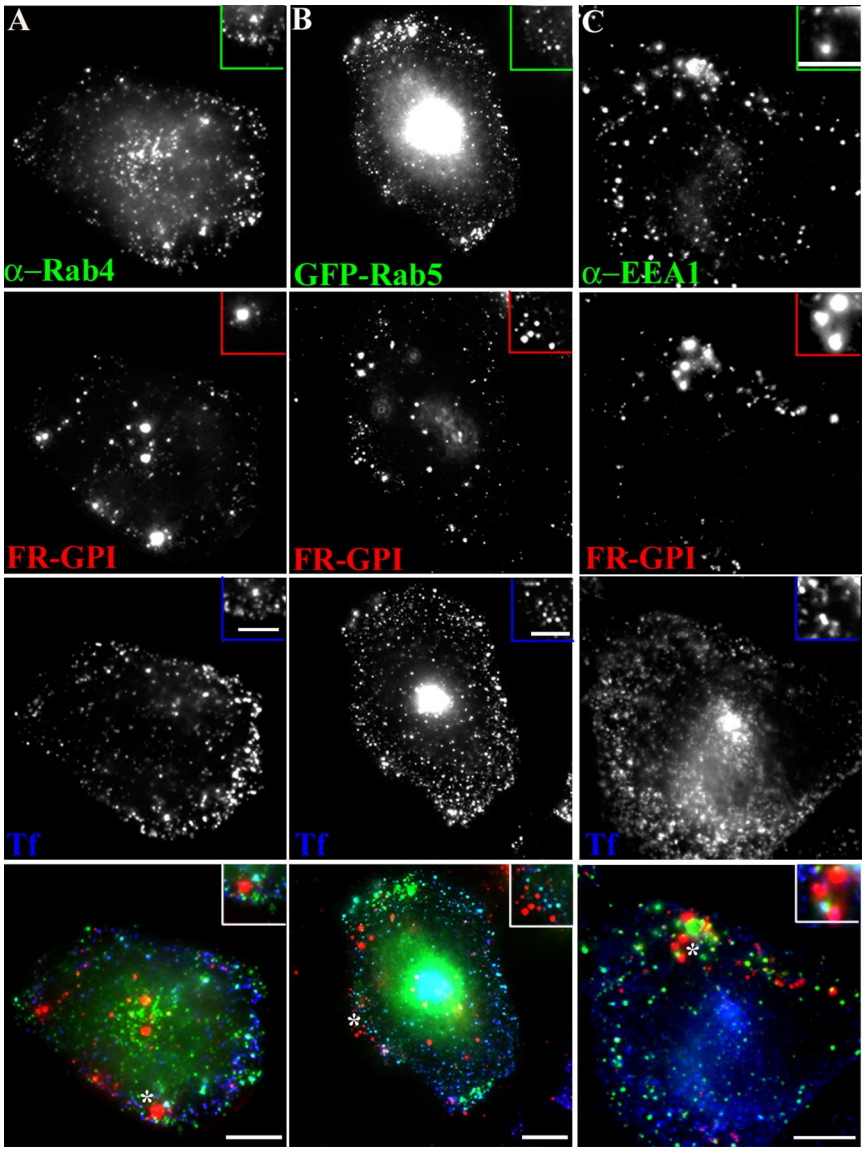

Figure 4. GPI-anchored proteins are internalized into GEECs devoid of early endosome markers. Untransfected CHO cells (A and C) or GFP-Rab5-transfected cells (B) were pulsed with Cy5-Fab-Mov18 (red) and Cy3-Tf (blue) for 2 min at 37°C, fixed, and labeled with antibody against Rab4 (green in A) or EEA1 (green in C) or directly imaged for GFP-fluorescence (green in B). Images of anti-Rab4, GFP-Rab5, or anti-EEA1 (green), FR-GPI (red), Tf (blue) are presented as gray scale images and pseudocolored and color merged (bottom). Insets show a magnified view of the region corresponding to the asterisk (*). Bar, 10 μm and 5 μm (inset).

these endosomes using a ratiometric method (Dunn *et al.*, 1994). Our data show that newly formed GEECs, which have not yet fused with sorting endosomes, are extremely acidic (note orange endosomes in Figure 3C), spanning a range from 5.5 to 6.5 (median ~6.0); Dex-containing endosomes that are colocalized with endocytosed Tf are less acidic, with a median pH ~6.5 (note green endosomes in Figure 3C). To rule out the possibility that fluid endosomes acquire late endosomal markers, the following experiments were performed. First, cells were mildly fixed and the pH was then measured. The results were identical to those obtained in live cells. Second, a time course of overlap of GEECs with GFP-Rab7 showed that GEECs as marked by FITC-Dex (1 mg/ml) are negative for Rab7 (Sabharanjak *et al.*, 2002). Pulse and chase experiments showed that fluid phase-containing endosomes do not become Rab7 positive until a 20-min chase (our unpublished data). Thus, fluid-phase containing compartments considered for pH measurement are GEECs and not late endosomes. The fluorescence of compartments accessed by endocytosed PLF-labeled FR-GPI at 2 min is significantly enhanced (~2-fold) upon neutralizing endosomal pH by treatment with 10 μM nigericin, confirming that GPI-anchored proteins are also accessing the acidic milieu of these endosomes, soon after internalization (our unpublished data).

To rule out any resemblance of these GEEC with the pH-neutral caveosomes (Pelkmans *et al.*, 2001), we found that there was no overlap with either endogenous caveolin (our unpublished data) or with overexpressed caveolin in CHO cells at 2 min, and 5 min (Supplemental Figure 5), as also detailed previously (Sabharanjak *et al.*, 2002). Furthermore, immortalized MEFs derived from mice that lack Cav-1 form similar GEECs (Kirkham *et al.*, 2005; Figure 9). However, we cannot rule out the possibility that a small fraction of GPI-anchored proteins are delivered to caveolin-marked compartments at late time points.

GPI-anchored Proteins Are Internalized into GEECs, Largely Devoid of Early Endosome Markers Rab4, Rab5, and EEA1

We next characterized presence of markers of early endosomes on GEECs in CHO (Figures 4 and 5) and BHK cells (Supplemental Figure 6). As indicated above, after 2-min pulse, internalized GPI-anchored proteins are first detected

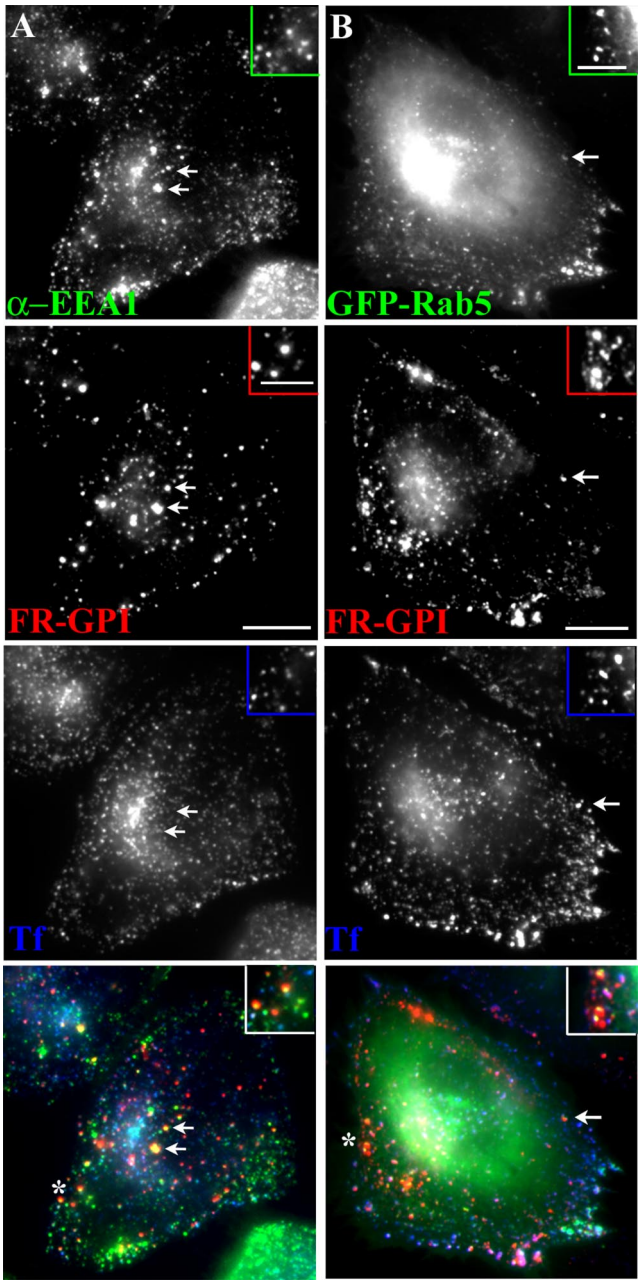

Figure 5. GEECs acquire Rab5 and EEA1 before fusion with sorting endosomes. (A and B) Untransfected CHO cells (A) or GFP-Rab5-transfected cells (B) were incubated for 5 min (A) or 10 min (B) with Cy5-Fab-Mov18 (red) and Cy3-Tf (blue) at 37°C, fixed, and labeled with antibody against EEA1 (green in A) or directly imaged for GFP fluorescence (green in B). Images were collected on a wide-field microscope, pseudocolored, and color merged. Insets show a magnified view of the regions corresponding to the asterisk (*). Bar, 10 μm and 5 μm (inset).

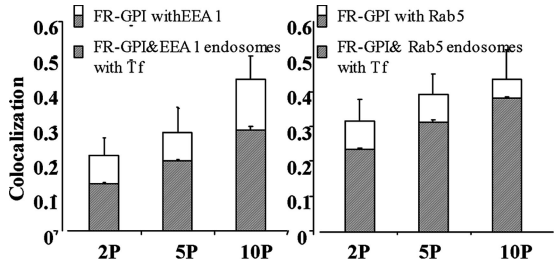

Figure 6. Kinetics of Rab5 and EEA1 loading on GEECs. FR-GPIs expressing cells were incubated with Cy5-Fab-Mov18 and Cy3-Tf and incubated at 37°C for different times (2P, 2 min; 5P, 5 min; and 10P, 10 min). Histogram shows quantitative extent of colocalization of Cy5-Fab-Mov18–positive endosomes with endogenous EEA1 (left) or GFP-Rab5 expressed in the same cells (right). The shaded area enclosed in the open bar indicates the fraction of Cy5-Fab-Mov18–positive endosomes that colocalized with both EEA1 and Tf (left) and with both GFP-Rab5 and Tf (right).

in GEECs, separate from Tf-containing sorting endosomes in a number of cell lines (Figures 3A and 4 and Supplemental Figure 6A; also see Sabharanjak *et al.*, 2002; Kirkham *et al.*, 2005). These structures did not colocalize with the endogenous sorting endosome marker Rab4 (Figure 4A) or exogenously expressed GFP-Rab4 (our unpublished data), which efficiently labeled the Tf-containing sorting endosomes at the same time (Figure 4A). GEECs also lack Rab5 at this time; there is very limited colocalization with GFP-Rab5 at 2 min after internalization (Figure 4B), whereas ≥50% of Tf-containing sorting endosomes are efficiently labeled with Rab5 at the same time point (Supplemental Figure 10). The majority of GEECs are also devoid of the early endosomal marker EEA1 in CHO (Figure 4C) and BHK cells (Supplemental Figure 6A).

To address the question of whether internalization of GPI-anchored proteins and fluid is dependent on the GTPase Rab5, we overexpressed wt, DA (Q71L mutant), and DN (S19N mutant) isoforms of GFP-Rab5 proteins (Supplemental Figure 7). As expected, DN-GFP-Rab5 inhibits Tf uptake via the clathrin-mediated pathway (our unpublished data; Bucci *et al.*, 1992). However, uptake of GPI-anchored proteins was not inhibited (Supplemental Figure 4). Indeed, there is occasionally an increase in uptake of GPI-anchored proteins in cells overexpressing DN-GFP-Rab5 (Supplemental Figure 7), similar to conditions when dynamin function is inhibited (Sabharanjak *et al.*, 2002; Guha *et al.*, 2003). These results strongly suggest that GEECs represent a separate endosomal population at the early time, whose biogenesis is independent of Rab4 or Rab5 activity.

GEECs Acquire Early Endosomal Markers in a PI3K-dependent Manner

In both CHO (Sabharanjak *et al.*, 2002; Figure 4) and BHK cells (Supplemental Figure 6A), GEECs are mainly devoid of early endosomal markers. They subsequently acquire Rab5 and EEA1 (Figure 5 and Supplemental Figure 6B). At 2 min, ~20% of the GEECs have EEA1, which increases to >40% by 10 min. After a 10-min pulse, many more GEECs become positive for EEA1 (Figure 6, left). Similar kinetics is observed for GFP-Rab5 loading on the GEECs (Figure 6, right). The extent of colocalization of GEECs with Tf-containing structures also increases with time (Figure 8D). Similar results are obtained in BHK cells (Supplemental Figure 6).

There could be two explanations for the loading of EEA1 and Rab5 on GEECs. One possibility is that GEECs acquire EEA1 (and Rab5) after they fuse with early endosomal marker-positive Tf-containing sorting endosomes, and the other possibility is that they acquire these proteins independent of fusion. Careful examination of GEECs that have not yet fused with Tf-containing sorting endosomes indicates that a significant portion of these endosomes contain detectable EEA1 and Rab5 (Figure 5, A and B, insets, arrows). Quantitative analysis of the extent of colocalization of FR-GPI with

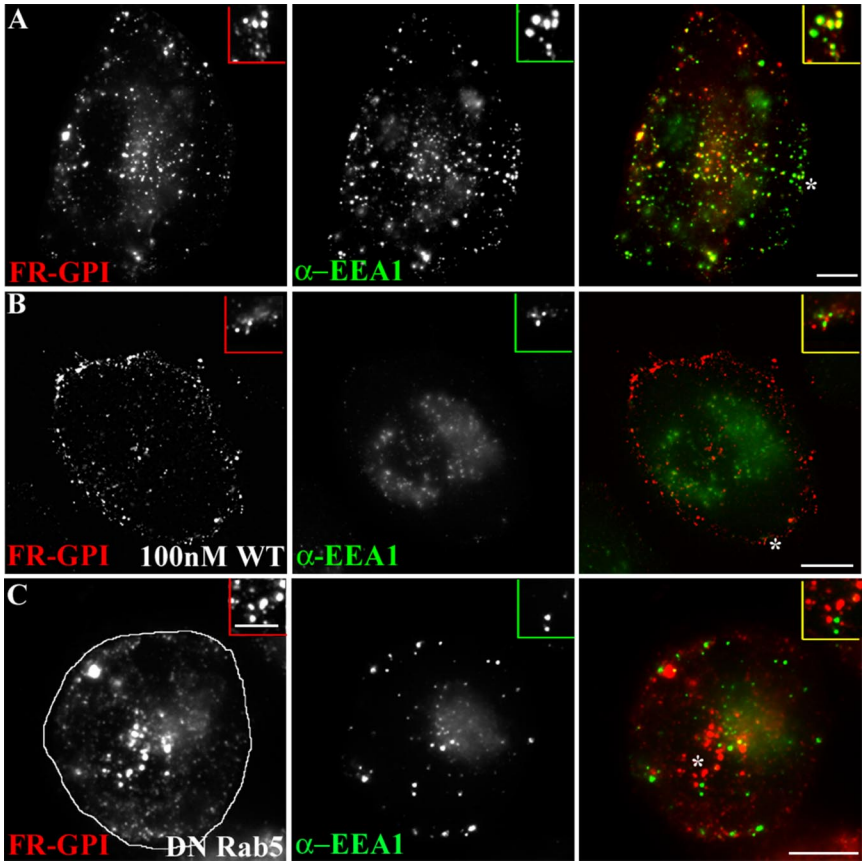

Figure 7. EEA1 loading on GEECs is prevented by PI3K and Rab5 inhibition. CHO cells either untreated (A) or pretreated (B) with 100 nM WT for 30 min. Cells were given a 10-min pulse of Cy5-Fab-Mov18 (red) followed by fixation, permeabilization and staining for EEA1 (green). (C) CHO cells, transfected with DN-GFP-Rab5 (outlined cell in C, left) were pulsed for 5 min with Cy5-Fab-Mov18 (red) followed by fixation, permeabilization, and staining for EEA1 (green). Images were pseudocolored and color combined. Note EEA1 fails to load on 5- or 10-min structures containing endocytosed GPI-anchored proteins. Insets show a magnified view of the regions corresponding to the asterisk (*). Bar, 10 μm and 5 μm (inset).

EEA1 and GFP-Rab5 shows that ~70% of the EEA1-positive and 80% of the GFP-Rab5-positive FR-GPI endosomes contain endocytosed Tf; the remaining 20–30% may acquire EEA1 and Rab5 independently of detectable Tf (Figure 6). These results suggest that EEA1 and Rab5 may be directly loaded onto GEECs, before fusion.

EEA1 is a key molecule involved in homotypic fusion between early endosomes (Mills *et al*., 1998; Simonsen *et al*., 1998). The C terminus of EEA1 contains a FYVE finger domain that binds to phosphatidylinositol-3-phosphate (PI3P) (Mu *et al*., 1995). In addition, it has two binding sites for the GTP-bound form of Rab5, one at the N-terminal zinc finger and one at the C terminus just upstream of the FYVE domain. Because the PI3P binding FYVE domain is nested within the Rab5 binding site, both PI-3 kinase and Rab5 activities are required for early endosome fusion. Studies have shown that Rab5 can recruit PI3Ks (Christoforidis *et al*., 1999b), including hVPS34 (Schu *et al*., 1993), and generate PI3P on the endosomal membrane. Together, PI3P and active Rab5-GTP synergize to generate a favorable environment for binding of EEA1 (Zerial and McBride, 2001).

On the sorting endosome, EEA1 is rapidly released from endosomal membranes in response to inhibition of PI3K activity by wortmannin (WT) treatment (Patki *et al*., 1997). WT is a fungal metabolite that specifically inhibits PI3K activity at low concentrations (Wymann *et al*., 1996). Treatment of CHO cells with low concentration of WT (100 nM) also prevents EEA1 loading on all early endosomal compartments; both Tf-containing sorting endosomes (our unpublished data) and GEECs are devoid of EEA1 (compare Figure 7, A with B). WT pretreatment significantly decreased the degree of colocalization between the GPI-anchored proteins and Tf (compare Figure 8, A and B; quantification in Figure 8D) in CHO and BHK (Supplemental Figure 9) cells. However, internalization of the GPI-anchored protein FR-GPI and the fluid phase was not affected by 100 nM WT-treatment (our unpublished data). These results suggest that PI3K activity and potentially EEA1 loading on GEECs may be required for fusion between the two endosomal systems, the dynamin-independent GEECs and dynamin-dependent sorting endosomes. PI3K inhibition also seemed to alter the size distribution and localization of GEECs; these endosomes remained more peripheral and smaller than their untreated counterparts (compare GEECs in Figure 7A with those in B, and Figure 8A with those in B). Furthermore, PI3K inhibition prevented homotypic fusion between GEECs (Supplemental Figure 8). However, WT treatment did not alter the acidic nature of these compartments. The fluorescence of compartments accessed by endocytosed PLF-labeled FR-GPI at 2 min in WT-treated cells was significantly enhanced (~2-fold) upon neutralizing endosomal pH by treatment with 10 μM nigericin (our unpublished data). These results confirm that GPI-anchored proteins endocytosed into an acidic environment even under conditions where fusion with other endosomes is inhibited.

These results suggest that the detection of early endosomal proteins, Rab5, and its effectors, EEA1, may have a functional significance in addition to facilitating heterotypic fusion with the sorting endosomes. These molecular players, especially EEA1 and PI3Ks may also mediate homotypic fusion between GEECs.

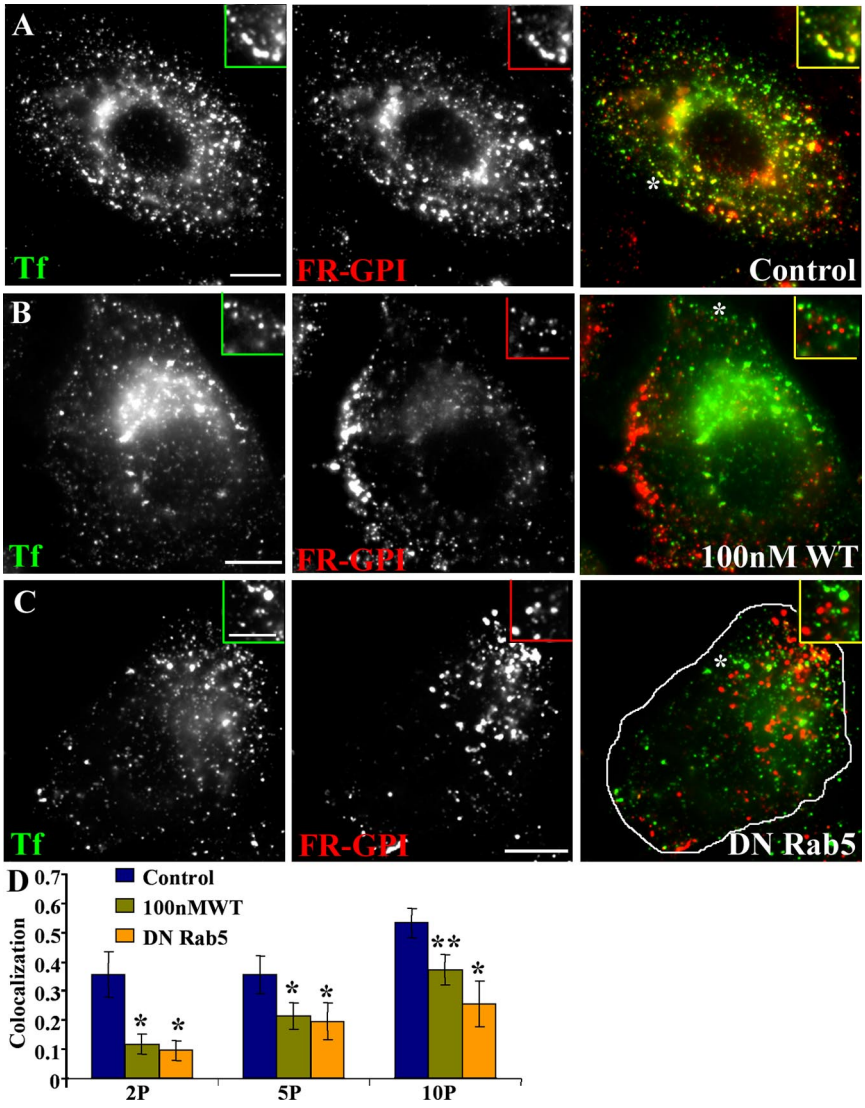

Figure 8. Inhibition of PI3K and Rab5 activity block mixing between GEECs and sorting endosomes. Control CHO cells (A), cells pretreated with 100 nM WT (B), or transfected with DN Rab5 (outlined cell in C) were pulsed for 10 min with Cy5-Fab-Mov18 (red) and Cy3-Tf (green), fixed, and imaged. Images were pseudocolored and color combined. Insets show a magnified view of the regions corresponding to the asterisk (*). (D) The extent of colocalization between Cy5-Fab-Mov18-containing (GEECs) and Tf-containing (sorting) endosomes was quantified at different pulse times (2P, 2 min; 5P, 5 min; and 10P, 10 min) for the different treatments as indicated by colored bars (untreated, purple; 100 nM WT, olive green; and DN-Rab5, orange). Colocalization index between FR-GPI and Tf is significantly different between cells treated with 100 nM WT and DN-Rab5 compared with control cells. *$p < 0.001$ and **$p < 0.003$, obtained from Student's t test comparing different data sets. Bar, 10 μm and 5 μm (inset).

GEEC Pathway in Cav1−/− MEFs

Recent studies have shown that a significant fraction of the CTxB uptake in Cav1−/− MEFs takes place via GEECs (or CLICs) in a caveolin-, clathrin-, and dynamin-independent pathway (Kirkham *et al.*, 2005). Ultrastructural identification demonstrated tubular/ring-like structures that budded from the plasma membrane (PM) as the major carriers involved in nonclathrin, noncaveolar uptake of CTxB in Cav1+/+ and Cav1−/− MEFs (Kirkham *et al.*, 2005). These tubular carriers were also found to be involved in endocytosis of GPI-anchored proteins. Here, we examined the kinetics of the GEEC pathway in immortalized MEFs derived from caveolin null mice. We find that the GEEC pathway functions similarly in both Cav1+/+ (Figure 9A) and Cav1−/− MEFs (Figure 9B). The extent of colocalization between GEECs marked by endocytosed antibodies to transfected CFP-GPI, and Tf is similar to that seen in CHO cells (Figure 9D, left). Furthermore, fusion between GEECs and Tf-positive endosomes remained sensitive to inhibition by 100 nM WT. Consistent with previous studies (Kirkham *et al.*, 2005), a significant fraction of CTxB uptake is colocalized with GEECs, and with Tf-containing endosomes (Figure 9D, right). Approximately, 50% of the endocytosed CTxB is in GEECs. This fraction decreases in WT-treated cells in Cav1−/− MEFs (Figures 8D and 9D, middle and right), identical to that observed in caveolin-positive cells (Cav1+/+ MEFs; our unpublished data). These results reiterate that both GPI-anchored protein and CTxB uptake via GEECs occurs in a similar manner in Cav1−/− cells, and undergo subsequent fusion with sorting endosomes via a PI3K-dependent mechanism. These results do not imply that all CTxB uptake occurs via GEECs, but they substantiate earlier evidence that a significant fraction (~50%) of this toxin enters cells via GEECs (Kirkham *et al.*, 2005).

Dominant-Negative Rab5 Inhibits Fusion between GEECs and Sorting Endosomes

The mechanism of EEA1 recruitment on sorting endosomes is dependent on both active Rab5 and PI3P generation (Christoforidis *et al.*, 1999b). The Rab5 GTPase forms a domain by recruiting hVps34, causing localized production of PI3P (Christoforidis *et al.*, 1999a). EEA1 stabilization on the GEECs also requires active Rab5 (Murray *et al.*, 2002). In cells overexpressing the DN-GFP-Rab5 mutant, EEA1 did not load on either the GEECs (Figure 7C) or sorting endosomes

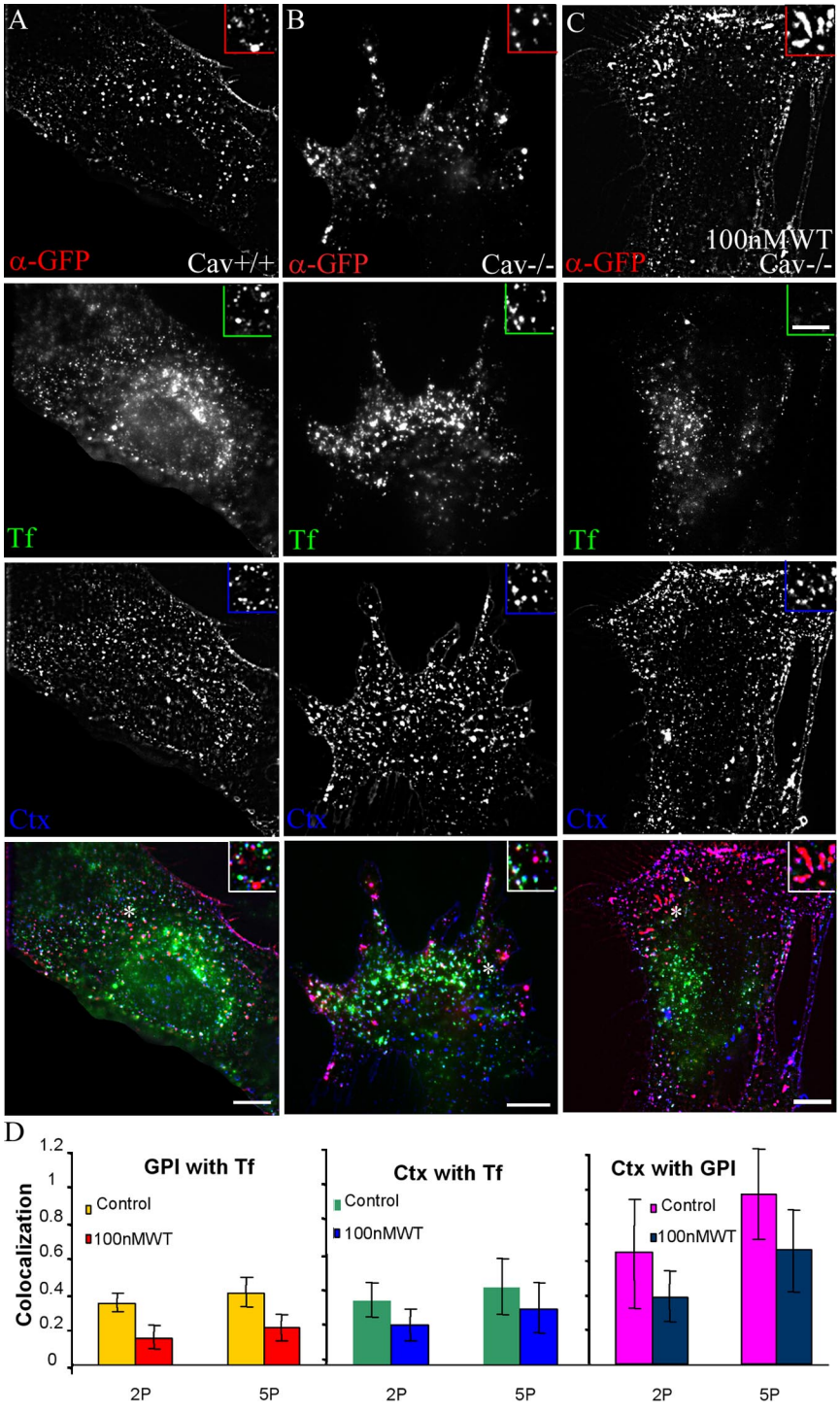

Figure 9. GEEC fuse with early sorting endosome with similar kinetics and in a PI3K-sensitive manner in Cav1−/− mouse embryonic fibroblasts. Mouse embryonic fibroblasts with and without caveolin expression were transfected with CFP-GPI. A 5-min pulse of Alexa 488 CTxB (blue); Alexa 568-anti-GFP-Fab (red), and Cy5-Tf (green) was given to Cav+/+ MEFs (A), Cav−/− MEFs (B), and Cav−/− MEFs (C) pretreated with 100 nM WT for 30 min. Images were pseudocolored, and color combined as described. Insets show a magnified view of the regions corresponding to the asterisk (*). (D) Histogram showing extent of colocalization between GPI and Tf, CTxB and Tf, and CTxB and GPI. Note that a significant fraction of endocytosed CTxB is internalized with CFP-GPI. Bar, 10 μm and 5 μm (inset).

(our unpublished data). These data indicate that Rab5 activity is required for EEA1 stabilization on the early endosomes of the GEEC and the sorting endosomal pathway. In cells expressing DN-GFP-Rab5, cargo from the two pathways also did not mix significantly at early time points (Figure 8C; quantification in D), suggesting that Rab5 activity and EEA1 stabilization is necessary for this fusion. In apparent contrast to WT-treated cells (Figure 8B), in DN-Rab5-expressing cells (Figure 8C), GEECs consistently occur more perinuclear and are larger than their untreated counterparts (Figure 8A) at the same time.

Overexpression of Rab5 Reverses WT-induced Inhibition of Fusion between GEECs and Sorting Endosomes by Recruiting EEA1

To further dissect the mechanism by which Rab5 and PI3P could mediate fusion between GEECs and sorting endosomes, we overexpressed GFP-Rab5wt in cells and treated them with 100 nM WT. Overexpression of GFP-Rab5, restores EEA1 loading on the Tf-containing endosomes (Figure 10A) as well as on the GEECs (Figures 10B and 11). In this background, fusion between the GEECs and sorting

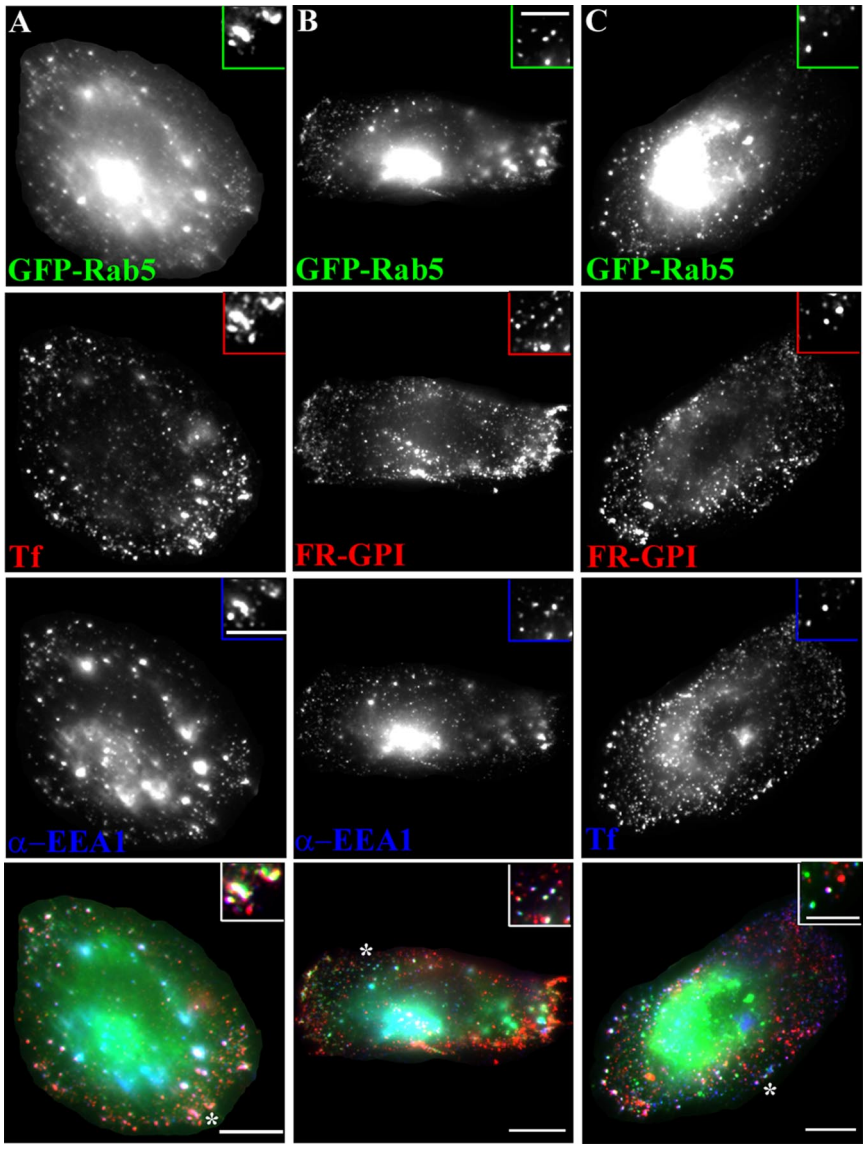

Figure 10. Overexpression of GFP-Rab5 can restore EEA1 loading and rescue fusion in WT-treated cells. CHO cells transfected with GFP-Rab5 (green) were pretreated with 100 nM WT for 30 min followed by pulse of Alexa 568-Tf (red in A, blue in C) and Cy5-Fab-Mov 18 (red in B and C) for 10 min. Cells were fixed, stained for EEA1 (blue in A and B), or directly imaged (C). Images were pseudocolored and color merged as described. Insets show a magnified view of the regions corresponding to the asterisk (*).

endosomes can take place (Figure 10C; quantitation Figure 11); the extent of fusion between GEECs and sorting endosomes were restored to levels indistinguishable from control levels (Figure 11). The results clearly indicate that in the presence of WT, increasing the level of Rab5 beyond endogenous levels can restore EEA1 loading on endosomes, and this correlates with restoration of fusion between these two endosomal systems. Together, these results provide evidence that recruitment of both EEA1 and Rab5 on the GEECs is necessary for fusion with Tf-containing sorting endosomes.

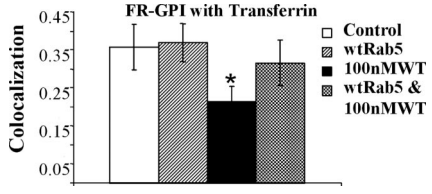

Figure 11. GFP-Rab5 overexpression can rescue fusion between GEECs and sorting endosomes. Histogram shows the extent of colocalization between GEECs and sorting endosomes as described in *Materials and Methods*. Colocalization index between FR-GPI and Tf in cells transfected with wtRab5, (with and without WT treatment) was not statistically different from control cells; p values ~0.3, whereas treatment with WT alone was significantly different from control or GFP-Rab5 expressing cells (*$p < 0.0001$, obtained from Student's *t* test by comparing the different data sets. Bar, 10 μm and 5 μm (inset).

DISCUSSION

Dynamin-independent pathways seem to be the main means by which GPI-anchored proteins and other membrane cargo that lack obvious localization signals are internalized. Although there are reports of internalization of GPI-anchored proteins via caveolae (Nichols, 2002; Peters *et al*., 2003), our results show that the caveolar pathway does not seem to be the major pathway for endocytosis of a majority of GPI-anchored proteins in CHO and MEF cells, although the virus particle SV40 is internalized via a clathrin-, dynamin-, Arf6-independent pathway in cells that do not express caveolae (Damm *et al*., 2005). However, the virus does not colocalize

with EEA1, or dextran and resides in a pH-neutral compartment. Therefore, the endosomes accessed by SV40 are likely to be distinct from the GEECs. Unlike dynamin-dependent processes, clathrin- and caveolin-coated pit-mediated pathways, the itineraries of endocytosed cargo internalized without dynamin are yet to be characterized. In addition to providing a description of a pathway, the temporal and spatial dynamics of the endosomes involved provide an understanding of the mechanism underlying the generic processes of endosome biogenesis and consumption.

Arf6-independent GPI-anchored Protein Endocytosis

The results presented here indicate that there are at least two types of dynamin-independent mechanisms, one type that is marked by Arf6, as described by Donaldson and colleagues in HeLa cells (Naslavsky *et al*., 2003, 2004), and the other type Arf6-independent. In contrast to the endocytic process involved in the uptake of GPI-anchored proteins (and other membrane components) in HeLa cells, we find that neither activating nor inactivating mutants of exogenously expressed Arf6 significantly alter GPI-anchored protein and fluid phase uptake in CHO cells. Furthermore, ectopically expressed Arf6 does not specifically label these endosomes, although it labels endosomes that contain cargo from the clathrin-mediated pathway (Tf-positive endosomes) as well as endosomes that contain both markers. Expression of DN-Arf6 had only a mild inhibitory effect on endocytosis in HeLa cells (Radhakrishna *et al*., 1996) but none in CHO cells, suggesting that neither Arf6 activation nor inactivation is essential for internalization and trafficking through this pathway. HeLa cells exhibit a much slower endocytic uptake rate of GPI-anchored proteins and fluid phase compared with CHO and BHK cells. This uptake in turn is up-regulated simply by overexpression of Arf6 (Radhakrishna *et al*., 1996), unlike that seen in CHO cells.

Another distinguishing feature of the endocytic mechanisms of GPI-anchored proteins between HeLa and CHO cells is the response to treatment of cells with AlF. In CHO cells, GPI-anchored protein and fluid phase uptake is inhibited by treatment with AlF, whereas it seems unaffected in HeLa cells (Radhakrishna *et al*., 1996). However, AlF treatment of cells overexpressing Arf6 causes stimulation of the uptake of GPI-anchored proteins and the fluid phase cargo in both cell lines (via endosomes that are now positive for Arf6). Because AlF can activate many G proteins in inactive GDP-bound form (Sternweis and Gilman, 1982), this treatment is probably disturbing the GDP-GTP exchange cycle of several proteins, including ectopically expressed Arf6.

One explanation is that although Arf6 is present in CHO cells and can localize to certain types of endosomes (Tf-containing sorting endosomes), endogenous machinery for Arf6-dependent GPI-anchored protein endocytosis is actively suppressed; endogenous Arf6 activated in the presence of AlF is also not sufficient for stimulating this pathway. Thus, in CHO cells, GPI-anchored proteins are constitutively endocytosed by a mechanism that does not involve Arf6. However, upon appropriate hyperactivation of Arf6, Arf6-dependent pathways can be made operational in CHO cells. It is also possible that CHO cells lack an essential component of the Arf6-dependent machinery. Nevertheless, CHO and BHK cells permit a dissection of a dynamin-independent pathway that does not use Arf6 function.

GEEC Pathway Is Not a Conventional Macropinocytic Pathway

The GEEC pathway accounts for a major portion of fluid phase uptake in CHO cells but differs from conventional macropinocytosis. The pathway is cdc42 dependent and not Rac1 dependent (Sabharanjak *et al*., 2002). Treatment with 100 μM methyl isobutyl amiloride does not significantly inhibit fluid uptake (Supplemental Figure 11). Macropinocytosis is dependent on activation of PI3K and protein kinase C (PKC) via epidermal growth factor receptor (EGFR). CHO cells do not have endogenous EGFR and the possibility of epidermal growth factor-independent downstream activation of PI3K and PKC is eliminated by the fact that the pathway is not blocked by inhibitors of PI3K (our unpublished data) and also by calphostin (a general PKC inhibitor at both low [50 nM] and high [1 mM] concentrations; our unpublished data).

Phorbol esters have been shown to stimulate macropinocytosis and solute flow through macrophages (Swanson, 1989). Treatment of CHO cells with phorbol 12-myristate 13-acetate (10–100 nM) and overexpression of dominant-active Rac1 increases fluid uptake dramatically, suggesting that molecular machinery for PKC-induced macropinocytosis exists in CHO cells (Supplemental Figure 11; Sabharanjak 2002; Sabharanjak and Mayor, unpublished data). These macropinosomes are large structures that contain both GPI-anchored proteins as well as Tf (almost immediately after formation (Sabharanjak 2002; Sabharanjak and Mayor, unpublished data), suggesting that unlike GEECs, macropinosomes are not very selective for membrane components.

GEECs Are Acidic Early Endosomes That Undergo WT-sensitive Fusion with Sorting Endosomes

Ultrastructural identification demonstrated tubular/ring-like structures that budded from the PM as the major carriers involved in nonclathrin, noncaveolar uptake of CTxB in Cav1+/+ and Cav1−/− MEFs (Kirkham *et al*., 2005) and GFP-GPI in CHO cells (Sabharanjak *et al*., 2002). Newly formed fluid and GPI-anchored protein containing endosomes are visualized as independent structures, strongly suggesting that these structures are primary endocytic vesicles visualized in our electron micrscopy analysis. They subsequently undergo WT-sensitive homotypic fusion with each other to form the GEECs. GEECs then fuse with endosomes carrying cargo from the clathrin-mediated pathway. In addition, the pH of all the endosomes (primary endocytic structures and GEECs) that are accessed by GPI-anchored proteins and the fluid phase is remarkably acidic at 6.0. This is ~0.5 pH units lower than the corresponding value measured for sorting endosomes (Mukherjee *et al*., 1997) and implies there is an efficient acidification mechanism existing for the GEECs. This could have functional implications, for example, in the facilitation of efficient release of small molecule ligands such as folates brought into GEECs by binding to GPI-anchored folate receptors (Sabharanjak and Mayor, 2004).

Our results show that intracellular fusion of GEECs with sorting endosomes derived from clathrin-mediated endocytic pathways in CHO and BHK cells is regulated by Rab5 and its effectors. After formation, GEECs acquire both EEA1 and Rab5 in structures that are not yet positive for Tf. This seems to enable fusion of GEECs with sorting endosomes. But, the kinetics of Tf-containing sorting endosomes also suggests that there are two stages of early sorting endosome maturation (Supplemental Figure 10), one stage where endosomes have low or nonexistent GFP-Rab5 levels, and the

second stage where GFP-Rab5 levels are high. Indeed, Tf-containing endosomes show only a 40% overlap with GFP-Rab5 from a 2-min pulse, which increases to 55% overlap at 10 min (Supplemental Figure 10). Of the Tf-containing endosomes only ~30% contain FR-GPI cargo at 2 min. However, a majority of the colocalized endosomes (~75%) were positive for GFP-Rab5, suggesting that this endosomal population have a distinct molecular identity.

Overexpression of GFP-Rab5 increased colocalization of the two types of cargo, suggesting that Rab5 machinery is critical for fusion between GEECs and sorting endosomes. Consistent with this DN-Rab5 inhibits the mixing of GPI-anchored proteins with Tf. These results suggest that Rab5 is capable of regulating heterotypic fusion, i.e., of mixing endosomes derived from different endocytic processes, in addition to its function in homotypic fusion of endosomes derived from the clathrin pit-mediated endosomal system (Bucci *et al*., 1992; Simonsen *et al*., 1998). However, distinct from the role of Rab5 in the generation of sorting endosomes via regulating coated vesicle formation and fusion with sorting endosomes (Bucci *et al*., 1992), inhibition of Rab5 function does not seem to have a role in the formation of GEECs.

PI3K and Cellular Localization of GEECs

PI3K is a potent Rab5 effector present on early endosomes, involved in building the feed-forward network necessary for generation of the putative Rab5 microdomain (Christoforidis *et al*., 1999b; Murray *et al*., 2002); WT blocks homotypic fusion by inhibiting the generation of PI3P, thereby inhibiting the recruitment of FYVE-domain containing EEA1 to membranes. Fusion of GEECs with sorting endosomes is blocked by inhibition of PI3K activity by WT, but uptake of GPI-anchored proteins is quantitatively unaffected. These observations suggest that the role of Rab5 in heterotypic fusion is also to effect stabilization of the Rab5-fusion effector EEA1. Overexpression of Rab5 in WT-treated cells leads to a restoration of fusion, coincident with a stabilization of EEA1 on the endosomal membrane. These results suggest a mechanism where the level of EEA1 recruitment is important for correct targeting during heterotypic fusion. Inhibition of PI3K activity also inhibits fusion between GEECs, suggesting that similar machinery may function in effecting fusion between GEECs.

Zerial and coworkers (Hoepfner *et al*., 2005) have recently shown that PI3P generation is not only accompanied by the recruitment of EEA1 but also regulates the loading of the pleckstrin homology domain bearing Kinesin family protein KIF16B. KIF16B is a plus-end–directed motor and mediates transport of early endosomes along microtubules; therefore, it regulates the steady-state distribution of early endosomes (Hoepfner *et al*., 2005). On treatment of cells with WT (similar to RNA interference-mediated silencing of KIF16B), Tf-containing endosomes move to the perinuclear region, this relocation is mimicked by DN-Rab5 inhibition of PI3K activation on sorting endosomes. GEECs seem to respond differently to these treatments; PI3K inhibition keeps "unfused" GEECs peripherally located, whereas DN-Rab5 expression seems to permit accelerated perinuclear relocation. Given the role of PI3P in localizing KIF16B, these observations would suggest that motors operating on the GEECs are under the control of other molecular players.

Implications for Trafficking via GEEC

The results presented here suggest a simple model for acidic GEEC formation and consumption, consistent with all available data. GEECs form via fusion between primary endocytic vesicles derived by a dynamin-independent mechanism, and occur as acidic fluid-containing endosomes carrying specialized membrane cargo. This occurs via a cdc42-dependent process, independent of Arf6 function. GEECs then undergo heterotypic fusion with sorting endosomes and potentially homotypic fusion with other GEECs by recruiting the familiar Rab5 fusion machinery. This involves Rab5 activation and EEA1 recruitment.

Inhibition of fusion between sorting endosomes and the GEEC pathway confirms previous observations that the two pathways indeed have very different cargo; at most ~10% of internalized GPI-anchored proteins are found in Tf-containing endosomes upon inhibition of PI3K. These results suggest that there is efficient segregation of molecules internalized via the two endocytic systems at the cell surface (Sabharanjak *et al*., 2002) and that GPI-anchored proteins are predominantly internalized via GEECs. In untreated cells, even at 2 min there is a detectable enhancement in mixing of GPI-anchored proteins and Tf, indicating that fusion of GEECs with sorting endosomes must occur very soon after formation. These observations also raise the question about how such an efficient segregation of GPI-anchored proteins is maintained in the face of the multitude of endocytic pathways available to membrane components at the cell surface.

At the same time, several questions still remain regarding the formation and consumption of GEECs. Foremost in the context of this study are questions governing the recruitment machinery for the loading of Rab5 onto GEECs. In the clathrin-dependent pathway, it is thought that Rab5 is loaded at multiple steps by the availability Rab5 GEFs at all stages in the endocytic process, from endocytic vesicles to sorting endosomal structures (Rubino *et al*., 2000). The guanine nucleotide exchange factors or membrane-associated recruitment factors that facilitate Rab5 loading onto GEECs are as yet undiscovered. Molecular regulators that effect Arf-6-independent, dynamin-independent pathways are also uncharacterized. Finally, understanding why (and how) different cell types such as CHO and BHK, after mixing their cargo from the dynamin-dependent and -independent pathways, segregate the same, kinetically in recycling endosomes in CHO (Sabharanjak *et al*., 2002), and to late endosomes in BHK cells (Fivaz *et al*., 2002), also remains an open question.

ACKNOWLEDGMENTS

We thank M. Zerial for Rab5 constructs; J. Donaldson for Arf6 constructs,V. Sriram for valuable suggestions, Gagan Gupta for critically reading the manuscript, and other members of the Mayor laboratory for generous help. Confocal microscopy was carried out in the Wellcome Trust-aided imaging facility at National Centre for Biological Sciences (Bangalore, India), supervised by H. Krishnamurthy. This work is supported by a Fast Track Fellowship for Young Scientists (Department of Science and Technology [DST], India) to M. K., a DST Swarnjayanti Fellowship (India) to S. M., and an R01 grant from the National Institutes of Health (United States) to R.G.P. S. M. acknowledges M. I. Sanity, K. Belur, and F. F. Bosphorus for inspiration.

REFERENCES

Anderson, R. G., Kamen, B. A., Rothberg, K. G., and Lacey, S. W. (1992). Potocytosis: sequestration and transport of small molecules by caveolae. Science *255*, 410–411.

Brown, F. D., Rozelle, A. L., Yin, H. L., Balla, T., and Donaldson, J. G. (2001). Phosphatidylinositol 4,5-bisphosphate and Arf6-regulated membrane traffic. J. Cell Biol. *154*, 1007–1018.

Bucci, P., Parton, R. G., Mather, I. H., Stunnenberg, H., Simons, K., Hoflack, B., and Zerial, M. (1992). The small GTPase rab5 functions as a regulatory factor in early endocytic pathway. Cell *70*, 715–728.

Chatterjee, S., and Mayor, S. (2001). The GPI-anchor and protein sorting. Cell Mol. Life Sci. *58*, 1969–1987.

Chatterjee, S., Smith, E. R., Hanada, K., Stevens, V. L., and Mayor, S. (2001). GPI anchoring leads to sphingolipid-dependent retention of endocytosed proteins in the recycling endosomal compartment. EMBO J. *20*, 1583–1592.

Christoforidis, S., McBride, H. M., Burgoyne, R. D., and Zerial, M. (1999a). The Rab5 effector EEA1 is a core component of endosome docking. Nature *397*, 621–625.

Christoforidis, S., Miaczynska, M., Ashman, K., Wilm, M., Zhao, L., Yip, S. C., Waterfield, M. D., Backer, J. M., and Zerial, M. (1999b). Phosphatidylinositol-3-OH kinases are Rab5 effectors. Nat. Cell Biol. *1*, 249–252.

Conese, M., Nykjaer, A., Petersen, C. M., Cremona, O., Pardi, R., Andreasen, P. A., Gliemann, J., Christensen, E. I., and Blasi, F. (1995). alpha-2 Macroglobulin receptor/Ldl receptor-related protein(Lrp)-dependent internalization of the urokinase receptor. J. Cell Biol. *131*, 1609–1622.

Conner, S. D., and Schmid, S. L. (2003). Regulated portals of entry into the cell. Nature *422*, 37–44.

D'Souza-Schorey C, Li, G., Colombo, M. I., and Sathl, P. D. (1995). A regulatory role for ARF6 in receptor-mediated endocytosis. Science *267*, 1175–1178.

D'Souza-Schorey, C., van Donselaar, E., Hsu, V. W., Yang, C., Stahl, P. D., and Peters, P. J. (1998). ARF6 targets recycling vesicles to the plasma membrane: insights from an ultrastructural investigation. J. Cell Biol. *140*, 603–616.

Damke, H., Baba, T., Warnock, D., and Schmid, S. (1994). Induction of mutant dynamin specifically blocks endocytic coated vesicle formation. J. Cell Biol. *127*, 915–934.

Damm, E. M., Pelkmans, L., Kartenbeck, J., Mezzacasa, A., Kurzchalia, T., and Helenius, A. (2005). Clathrin- and caveolin-1-independent endocytosis: entry of simian virus 40 into cells devoid of caveolae. J. Cell Biol. *168*, 477–488.

Donaldson, J. (2003). Multiple roles for Arf 6, sorting, structuring and signaling at the plasma membrane. J. Biol. Chem. *278*, 41573–41576.

Dunn, K. W., Mayor, S., Myers, J. N., and Maxfield, F. R. (1994). Applications of ratio fluorescence microscopy in the study of cell physiology. FASEB J. *8*, 573–582.

Dunn, K., McGraw, T., and Maxfield, F. (1989). Iterative fractionation of recycling receptors from lysosomally destined ligands in an early sorting endosome. J. Cell Biol. *109*, 3303–3314.

Fivaz, M., Vilbois, F., Thurnheer, S., Pasquali, C., Abrami, L., Bickel, P. E., Parton, R. G., and van der Goot, F. G. (2002). Differential sorting and fate of endocytosed GPI-anchored proteins. EMBO J. *21*, 3989–4000.

Ghosh, R., Gelman, D., and Maxfield, F. (1994). Quantification of low density lipoprotein and transferrin endocytic sorting HEp2 cells using confocal microscopy. J. Cell Sci. *107*, 2177–2189.

Gruenberg, J., and Maxfield, F. R. (1995). Membrane transport in the endocytic pathway. Curr. Opin. Cell Biol. *7*, 552–563.

Guha, A., Sriram, V., Krishnan, K. S., and Mayor, S. (2003). shibire mutations reveal distinct dynamin-independent and dependent endocytic pathways in primary cultures of *Drosophila* hemocytes. J. Cell Sci. *116*, 3373–3386.

Henley, J. R., Krueger, E.W.A., Oswald, B. J., and McNiven, M. A. (1998). Dynamin-mediated internalization of caveolae. J. Cell Biol. *141*, 85–99.

Hinshaw, J. E., and Schmid, S. L. (1995). Dynamin self-assembles into rings suggesting a mechanism for coated vesicle budding *374*, 190–192.

Hoepfner, S., Severin, F., Cabezas, A., Habermann, B., Runge, A., Gillooly, D., Stenmark, H., and Zerial, M. (2005). Modulation of receptor recycling and degradation by the endosomal kinesin KIF16B. Cell *121*, 437–450.

Honda, A., *et al*. (1999). Phosphatidylinositol 4-phosphate 5-kinase alpha is a downstream effector of the small G protein ARF6 in membrane ruffle formation. Cell *99*, 521–532.

Kirkham, M., Fujita, A., Chadda, R., Nixon, S. J., Kurzchalia, T. V., Sharma, D. K., Pagano, R. E., Hancock, J. F., Mayor, S., and Parton, R. G. (2005). Ultrastructural identification of uncoated caveolin-independent early endocytic vehicles. J. Cell Biol. *168*, 465–476.

Kirkham, M., and Parton, R. G. (2005). Clathrin-independent endocytosis: new insights into caveolae and non-caveolar lipid raft carriers. Biochim. Biophys. Acta *1745*, 273–286.

Lamaze, C., Dujeancourt, A., Baba, T., Lo, C. G., Benmerah, A., and Dautry-Varsat, A. (2001). Interleukin 2 receptors and detergent-resistant membrane domains define a clathrin-independent endocytic pathway. Mol. Cell *7*, 661–671.

Lamaze, C., and Schmid, S. L. (1995). The emergence of clathrin-independent pinocytic pathways. Curr. Opin. Cell Biol. *7*, 573–580.

Maxfield, F. R. (1989). Measurement of vacuolar pH and cytoplasmic calcium in living cells using fluorescence microscopy. Methods Enzymol. *173*, 745–771.

Mayor, S., Presley, J., and Maxfield, F. (1993). Sorting of membrane components from endosomes and subsequent recycling to the cell surface occurs by a bulk flow process. J. Cell Biol. *121*, 1257–1269.

Mayor, S., and Riezman, H. (2004). Sorting GPI-anchored proteins. Nat. Rev. Mol. Cell Biol. *5*, 110–120.

Mayor, S., Sabharanjak, S., and Maxfield, F. R. (1998). Cholesterol-dependent retention of GPI-anchored proteins in endosomes. EMBO J. *17*, 4626–4638.

McLauchlan, H., Newell, J., Morrice, N., Osborne, A., West, M., and Smythe, E. (1998). A novel role for Rab5-GDI in ligand sequestration into clathrin-coated pits. Curr. Biol. *8*, 34–45.

Mellman, I. (1996). Membranes and sorting. Curr. Opin. Cell Biol. *8*, 497–498.

Mills, I., Jones, A., and Clague, M. (1998). Involvement of the endosomal autoantigen EEA1 in homotypic fusion of early endosomes. Curr. Biol. *8*, 881–884.

Mu, F.-T., Callaghan, J. M., Steele-Mortimer, O., Stenmark, H., Parton, R. G., Campbell, P. L., McCluskey, J., Yeo, J.-P., Tock, E.P.C., and Toh, B.-H. (1995). EEA1, an early endosome-associated protein. J. Biol. Chem. *270*, 13503–13511.

Mukherjee, S., Ghosh, R. N., and Maxfield, F. R. (1997). Endocytosis. Physiol. Rev. *77*, 759–803.

Murray, J. T., Panaretou, C., Stenmark, H., Miaczynska, M., and Backer, J. M. (2002). Role of Rab5 in the recruitment of hVps34/p150 to the early endosome. Traffic *3*, 416–427.

Nabi, I. R., and Le, P. U. (2003). Caveolae/raft-dependent endocytosis. J. Cell Biol. *161*, 673–677.

Naslavsky, N., Weigert, R., and Donaldson, J. G. (2003). Convergence of non-clathrin- and clathrin-derived endosomes involves Arf6 inactivation and changes in phosphoinositides. Mol. Biol. Cell *14*, 417–431.

Naslavsky, N., Weigert, R., and Donaldson, J. G. (2004). Characterization of a nonclathrin endocytic pathway: membrane cargo and lipid requirements. Mol. Biol. Cell *15*, 3542–3552.

Nichols, B. J. (2002). A distinct class of endosome mediates clathrin-independent endocytosis to the Golgi complex. Nat. Cell Biol. *4*, 374–378.

Nichols, B. J. (2003). GM1-containing lipid rafts are depleted within clathrin-coated pits. Curr. Biol. *13*, 686–690.

Nykjaer, A., *et al*. (1992). Purified alpha 2-macroglobulin receptor/LDL receptor-related protein binds urokinase plasminogen activator inhibitor type-1 complex. Evidence that the alpha 2-macroglobulin receptor mediates cellular degradation of urokinase receptor-bound complexes. J. Biol. Chem. *267*, 14543–14546.

Oh, P., McIntosh, D. P., and Schnitzer, J. E. (1998). Dynamin at the neck of caveolae mediates their budding to form transport vesicles by GTP-driven fission from the plasma membrane of endothelium. J. Cell Biol. *141*, 101–114.

Palacios, F., Schweitzer, J. K., Boshans, R. L., and D'Souza-Schorey, C. (2002). ARF6-GTP recruits Nm23–H1 to facilitate dynamin-mediated endocytosis during adherens junctions disassembly. Nat. Cell Biol. *4*, 929–936.

Paleotti, O., Macia, E., Luton, F., Klein, S., Partisani, M., Chardin, P., Kirchhausen, T., and Franco, M. (2005). The small G-protein Arf6GTP recruits the AP-2 adaptor complex to membranes. J. Biol. Chem. *280*, 21661–21666.

Parton, R. G., Joggerst, B., and Simons, K. (1994). Regulated internalization of caveolae. J. Cell Biol. *127*, 1199–1215.

Patki, V., Virbasius, J., Lane, W. S., Toh, B.-H., Shpetner, H. S., and Corvera, S. (1997). Identification of an early endosomal protein regulated by phosphatidylinositol 3-kinase. Proc. Natl. Acad. Sci. USA *94*, 7326–7330.

Pauly, P. C., and Harris, D. A. (1998). Copper stimulates endocytosis of the prion protein. J. Biol. Chem. *273*, 33107–33110.

Pelkmans, L., Burli, T., Zerial, M., and Helenius, A. (2004). Caveolin-stabilized membrane domains as multifunctional transport and sorting devices in endocytic membrane traffic. Cell *118*, 767–780.

Pelkmans, L., Kartenbeck, J., and Helenius, A. (2001). Caveolar endocytosis of simian virus 40 reveals a new two-step vesicular-transport pathway to the ER. Nat. Cell Biology *3*, 473–483.

Peters, P. J., *et al*. (2003). Trafficking of prion proteins through a caveolae-mediated endosomal pathway. J. Cell Biol. *162*, 703–717.

Pfeffer, S. R. (2001). Rab GTPases: specifying and deciphering organelle identity and function. Trends Cell Biol. *11*, 487–491.

Poussin, C., Foti, M., Carpentier, J. L., and Pugin, J. (1998). CD14-dependent endotoxin internalization via a macropinocytic pathway. J. Biol. Chem. *273*, 20285–20291.

Prigent, M., Dubois, T., Raposo, G., Derrien, V., Tenza, D., Rosse, C., Camonis, J., and Chavrier, P. (2003). ARF6 controls post-endocytic recycling through its downstream exocyst complex effector. J. Cell Biol. *163*, 1111–1121.

Radhakrishna, H., and Donaldson, J. G. (1997). ADP-ribosylation factor 6 regulates a novel plasma membrane recycling pathway. J. Cell Biol. *139*, 49–61.

Radhakrishna, H., Klausner, R. D., and Donaldson, J. G. (1996). Aluminum fluoride stimulates surface protrusions in cells overexpressing the ARF6 GTPase. J. Cell Biol. *134*, 935–947.

Razani, B., and Lisanti, M. P. (2001). Caveolin-deficient mice: insights into caveolar function human disease. J. Clin. Investig. *108*, 1553–1561.

Ricci, V., Galmiche, A., Doye, A., Necchi, V., Solcia, E., and Boquet, P. (2000). High cell sensitivity to. Helicobacter pylori VacA toxin depends on a GPI-anchored protein and is not blocked by inhibition of the clathrin-mediated pathway of endocytosis. Mol. Biol. Cell *11*, 3897–3909.

Rubino, M., Miaczynska, M., Lippe, R., and Zerial, M. (2000). Selective membrane recruitment of EEA1 suggests a role in directional transport of clathrin-coated vesicles to early endosomes. J. Biol. Chem. *275*, 3745–3748.

Sabharanjak, S., and Mayor, S. (2004). Folate receptor endocytosis and trafficking. Adv. Drug Deliv. Rev. *56*, 1099–1109.

Sabharanjak, S., Sharma, P., Parton, R. G., and Mayor, S. (2002). GPI-anchored proteins are delivered to recycling endosomes via a distinct cdc-42 regulated, clathrin-independent pinocytic pathway. Dev. Cell *2*, 411–423.

Schu, P. V., Takegawa, K., Fry, M. J., Stack, J. H., Waterfield, M. D., and Emr, S. D. (1993). Phosphatidylinositol 3-kinase encoded by yeast VPS34 gene essential for protein sorting. Science *260*, 88–91.

Sharma, P., Sabharanjak, S., and Mayor, S. (2002). Endocytosis of lipid rafts: an identity crisis. Semin. Cell Dev. Biol. *13*, 205–214.

Sharma, P., Varma, R., Sarasij, R. C., Ira, Gousset, K., Krishnamoorthy, G., Rao, M., and Mayor, S. (2004). Nanoscale organization of multiple GPI-anchored proteins in living cell membranes. Cell *116*, 577–589.

Simons, K., and Zerial, M. (1993). Rab proteins and the road maps for intracellular transport. Neuron *11*, 789–799.

Simonsen, A., Lippe, R., Christoforidis, S., Gaullier, J.-M., Brech, A., Callaghan, J., Toh, B.-H., Murphy, C., Zerial, M., and Stenmark, H. (1998). EEA1 links PI(3)K function to Rab5 regulation of endosome fusion. Nature *394*, 494–498.

Skretting, G., Torgersen, M. L., van Deurs, B., and Sandvig, K. (1999). Endocytic mechanisms responsible for uptake of GPI-linked diphtheria toxin receptor. J. Cell Sci. *112*, 3899–3909.

Song, J., Khachikian, Z., Radhakrishna, H., and Donaldson, J. (1998). Localization of endogenous ARF6 to sites of cortical actin rearrangement and involvement of ARF6 in cell spreading. J. Cell Sci. *111*, 2257–2267.

Sternweis, P. C., and Gilman, A. G. (1982). Aluminum: a requirement for activation of the regulatory component of adenylate cyclase by fluoride. Proc. Natl. Acad. Sci. USA *79*, 4888–4891.

Sunyach, C., Jen, A., Deng, J., Fitzgerald, K. T., Frobert, Y., Grassi, J., McCaffrey, M. W., and Morris, R. (2003). The mechanism of internalization of glycosylphosphatidylinositol-anchored prion protein. EMBO J. *22*, 3591–3601.

Swanson, J. A. (1989). Phorbol esters stimulate macropinocytosis and solute flow through macrophages. J. Cell Sci. *94*, 135–142.

Tanabe, K., Torii, T., Natsume, W., Braesch-Andersen, S., Watanabe, T., and Satake, M. (2005). A novel GTPase-activating protein for ARF6 directly interacts with clathrin and regulates clathrin-dependent endocytosis. Mol. Biol. Cell *16*, 1617–1628.

Triantafilou, K., Triantafilou, M., and Dedrick, R. L. (2001). A CD14-independent LPS receptor cluster. Nat. Immunol. *2*, 338–345.

Wymann, M., Bulgarelli-Leva, G., Zvelebil, M., Pirola, L., Vanhaesebroeck, B., Waterfield, M., and Panayotou, G. (1996). Wortmannin inactivates phosphoinositide 3-kinase by covalent modification of Lys-802, a residue involved in the phosphate transfer reaction. Mol. Cell Biol. *16*, 1722–1733.

Zerial, M., and McBride, H. (2001). Rab proteins as membrane organizers. Nat Rev Mol. Cell Biol. *2*, 107–117.